XV MPD Collaboration Meeting

15–17 | April | 2025

VBLHEP, JINR

Fluctuation Measurements from the RHIC Beam Energy Scan Program

Fan Si

University of Science and Technology of China

April 17, 2025

Outline

- 1. Introduction
- 2. Selected Results from BES-II
  - (Net-)Proton Fluctuations (7.7–27 GeV)
  - Proton Fluctuations (3.2–3.9 GeV)
- 3. Summary and Outlook

Introduction: QCD Phase Diagram

- Transition between hadronic ⇔ QGP phases
- Crossover at small μ_B ($\mu_B/T < 2$)
  - No distinct phase boundary
  - Expected by Lattice QCD
  - $T = 156.5 \pm 1.5$ MeV at $\mu_B = 0$
- First-order phase transition at higher μ_B
  - Predicted by QCD-based models
- Critical point (CP)?
  - Second-order phase transition
  - Conjectured to terminate first-order phase boundary

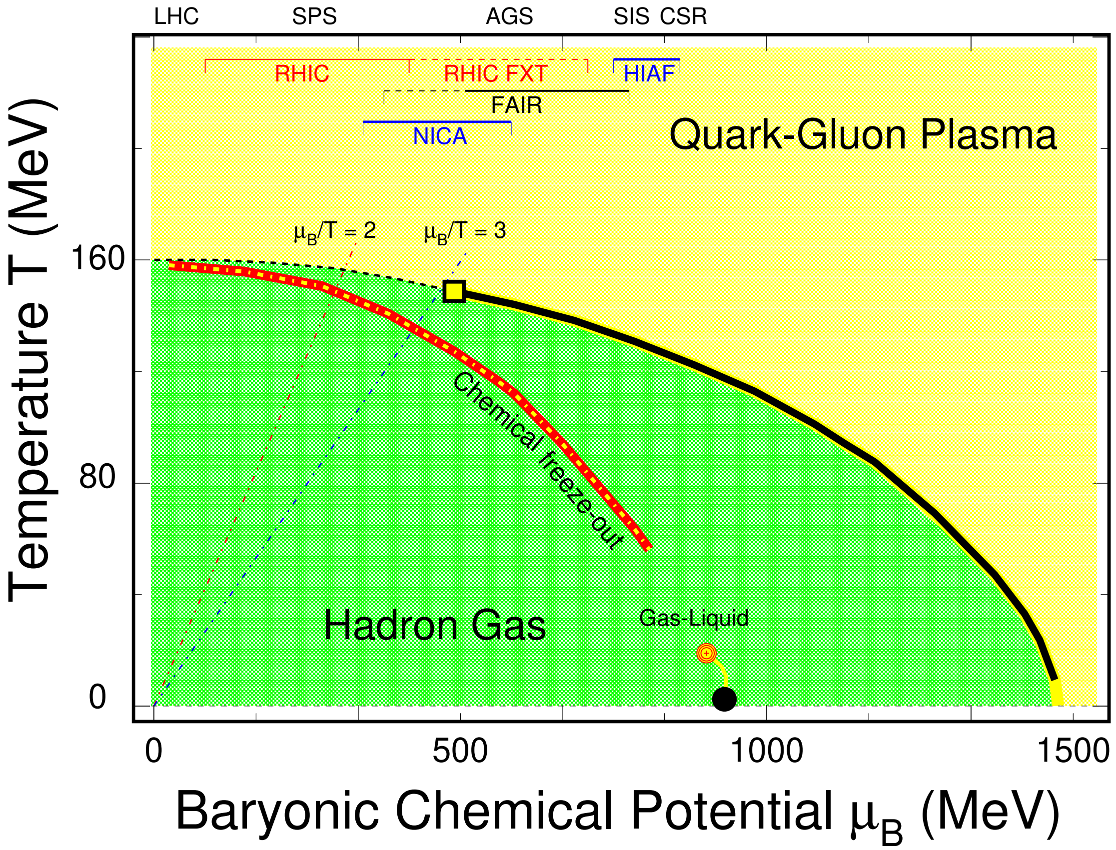

B. Mohanty, N. Xu, arXiv:2101.09210
Y. Aoki *et al.*, Nature 443, 675-678 (2006)
HotQCD, PLB 795, 15-21 (2019)

- Critical physics goal: search for and locate CP, understand QCD phase structure

Introduction: RHIC Beam Energy Scan Program

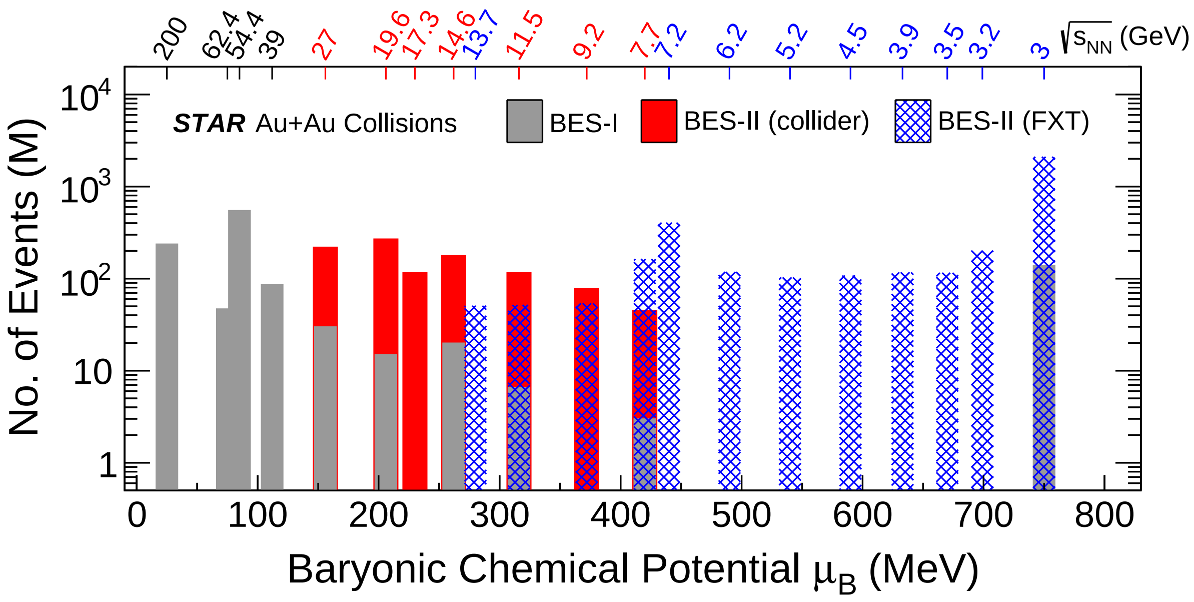

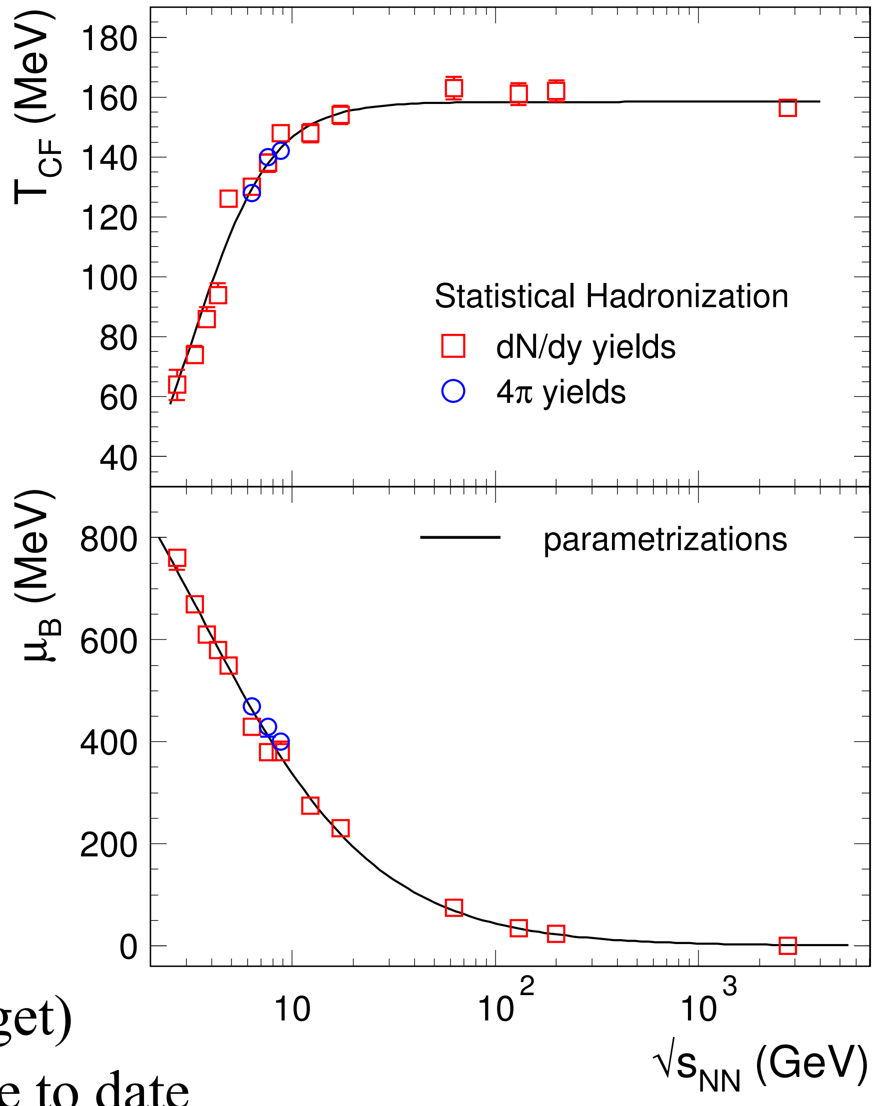

- Scan QCD phase diagram by varying $\sqrt{s_{\mathrm{NN}}}$
  - Low energy ⇒ low T, high μ_{B} at chemical freeze-out
- RHIC Beam Energy Scan (Au+Au)
  - BES-I (2010–2017): $\sqrt{s_{\mathrm{NN}}} = 7.7$–200 GeV
  - BES-II (2018–2021):
    - $\sqrt{s_{\mathrm{NN}}} = 7.7$–27 GeV (collider), 3–13.7 GeV (fixed-target)
  - $750 \gtrsim \mu_{\mathrm{B}}$ (MeV) $\gtrsim 25$: high precision, widest μ_{B} coverage to date

A. Andronic *et al.*, Nature 561, 321-330 (2018)

Introduction: STAR Detector System

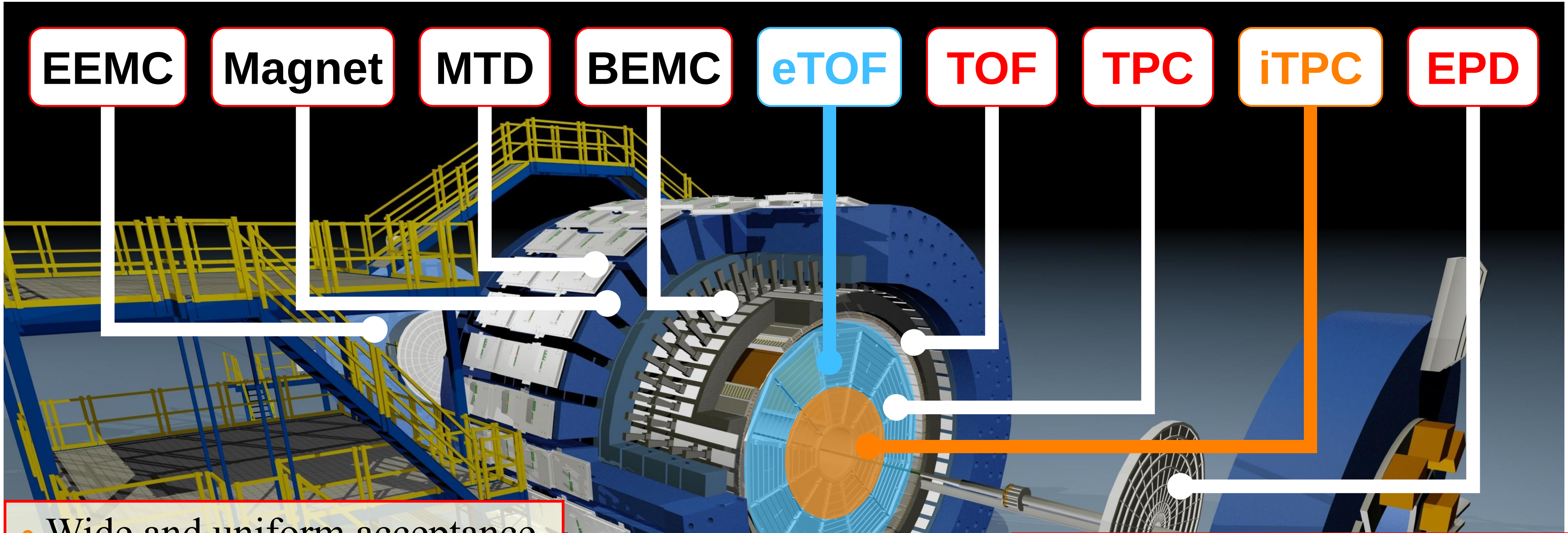

- Wide and uniform acceptance
- Excellent tracking and PID
- Modest rates
- Upgraded since 2018
  - EPD, iTPC, eTOF

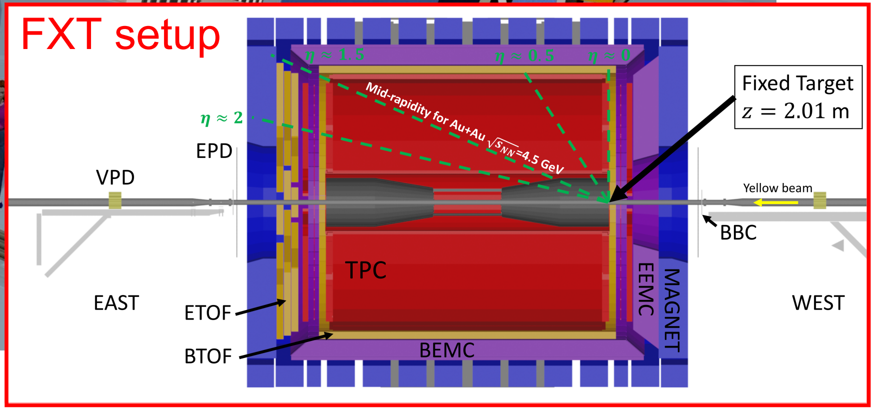

Introduction: STAR Major Upgrades for BES-II

Inner TPC (2019+)

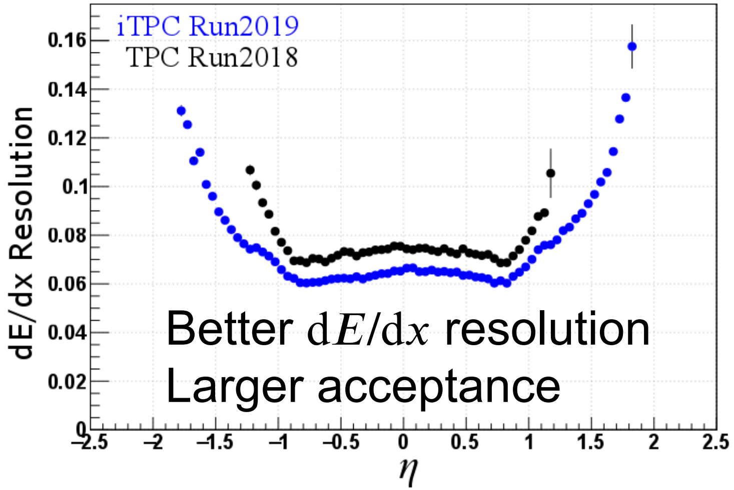

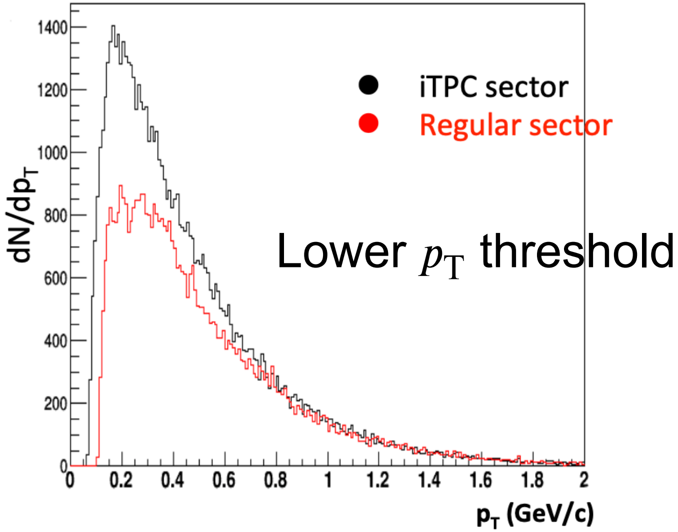

End-cap TOF (2019+)

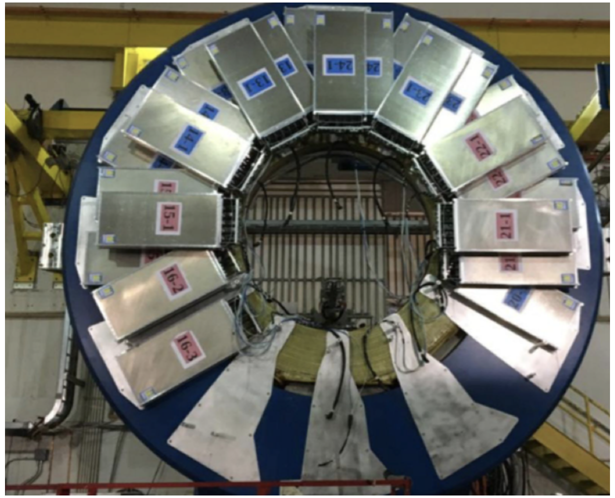

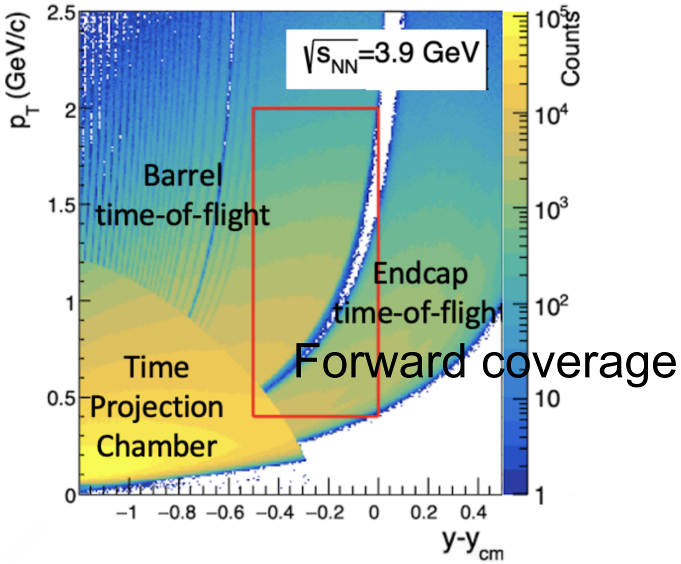

Event Plane Detector (2018+)

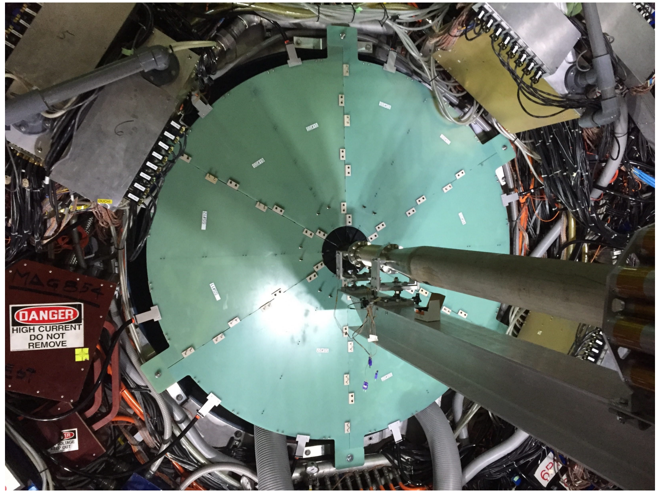

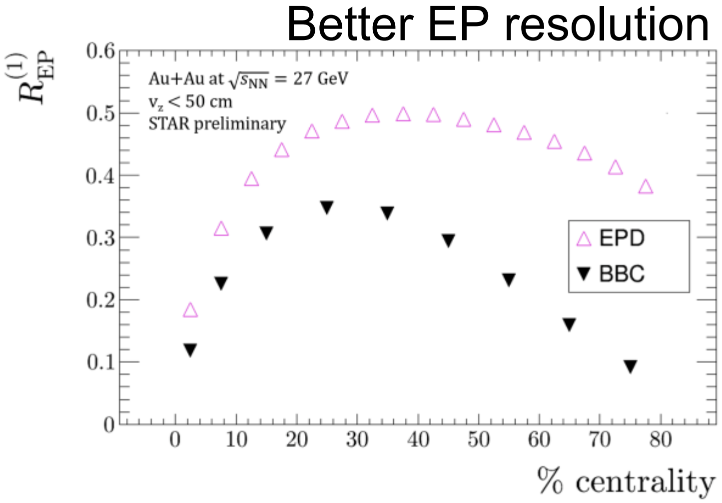

Y. Yang (STAR), NPA 1005, 121758 (2021)

Introduction: Observables

1. Expected divergence of correlation length ξ and susceptibility $\chi_{r,q}$ (for conserved charge q) at CP
2. N: E-by-E net-proton number as proxy for net-baryon number
3. Cumulants: (using $\mu_r = \langle (N - \langle N \rangle)^r \rangle$)
   - $C_1 = \mu \quad = \langle N \rangle$
   - $C_2 = \sigma^2 \quad = \mu_2$
   - $C_3 = S\sigma^3 = \mu_3$
   - $C_4 = \kappa\sigma^4 = \mu_4 - 3\mu_2^2$
   - $C_{r,q} \sim \xi^{5r/2-3} \Rightarrow$ higher orders are more sensitive
   - $C_{r,q}/C_{s,q} = \chi_{r,q}/\chi_{s,q} \Rightarrow$ trivial volume dependence canceled
4. Factorial cumulants:
   - $\kappa_1 = C_1$
   - $\kappa_2 = C_2 - C_1$
   - $\kappa_3 = C_3 - 3C_2 + 2C_1$
   - $\kappa_4 = C_4 - 6C_3 + 11C_2 - 6C_1$
   - Quantification of r-particle correlation by κ_r

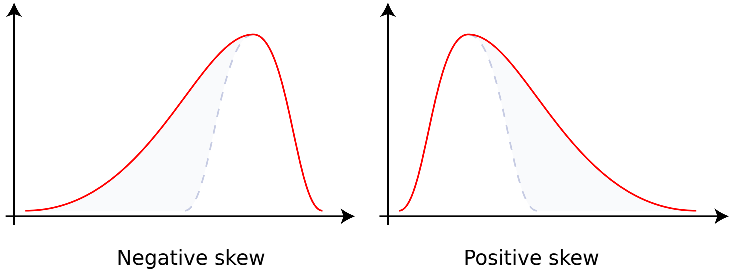

skewness $S = \mu_3/\sigma^3 \Leftrightarrow$ asymmetry

Gaussian: $C_r = 0$ $(r > 2)$
Poisson: $C_r = C_1$, $\kappa_r = 0$ $(r > 1)$
Skellam (Poisson − Poisson):
$$C_{\text{odd}}/C_{\text{odd}} = C_{\text{even}}/C_{\text{even}} = 1$$

kurtosis $\kappa = \mu_4/\sigma^4 - 3 \Leftrightarrow$ peakedness

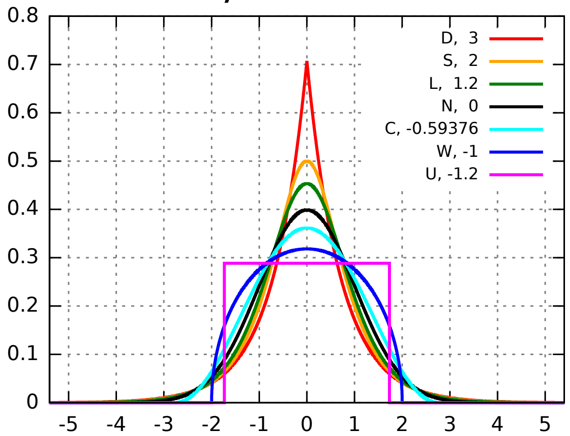

Introduction: Expected Signals

- Critical signal: non-monotonic energy dependence of C_4/C_2
  - ω_4: scaled C_4
  - Baseline: determined by models without CP

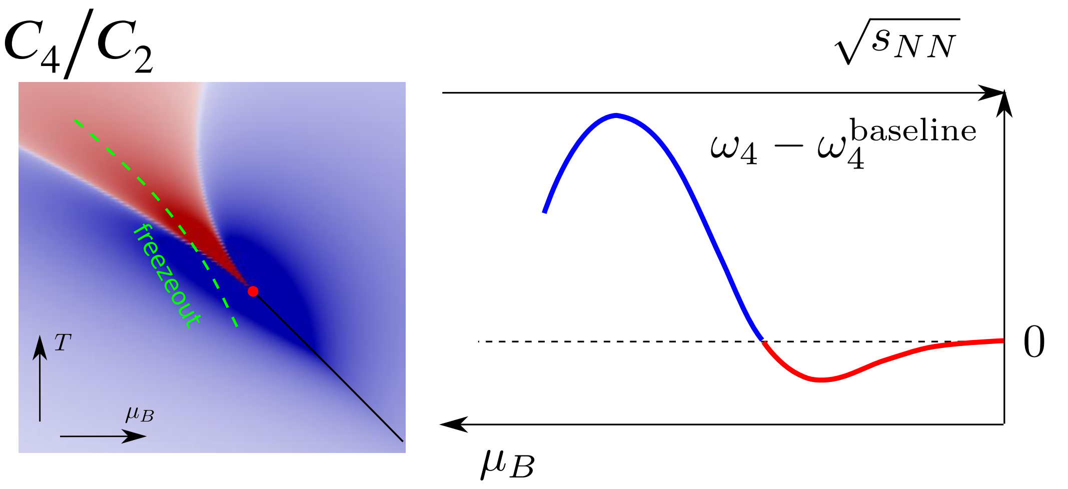

- Possible structures in acceptance dependence
  - $1/X$: acceptance; $\langle Q^r \rangle_c = C_{r,Q}$

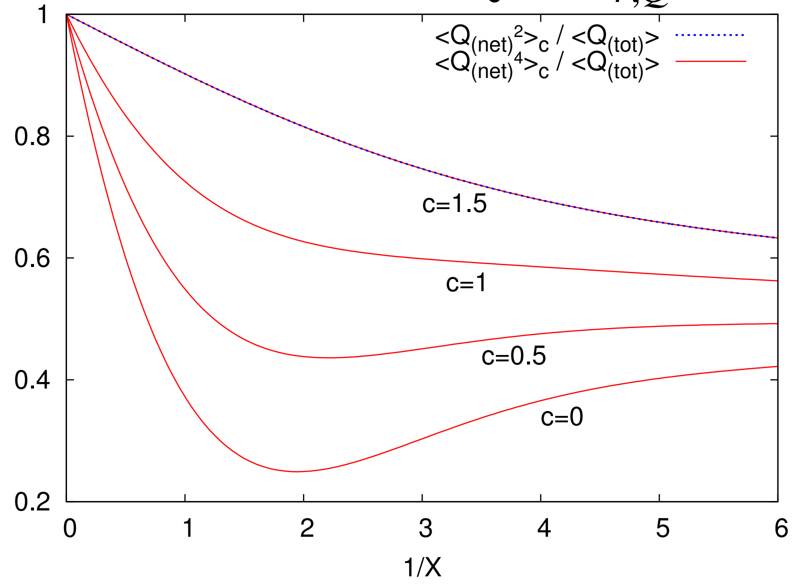

- Crossover signal: negative C_5 and C_6

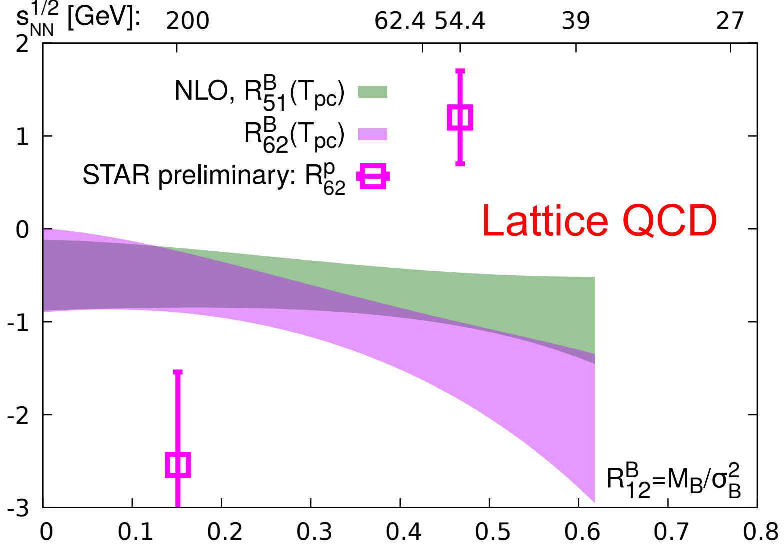

M. Kitazawa, M. Asakawa, H. Ono, PLB 728, 386-392 (2014)
A. Bazavov *et al.*, PRD 101, 074502 (2020)
M. Stephanov, Acta Phys. Polon. B 55, 5-A4 (2024)

Introduction: Previous Measurements at RHIC

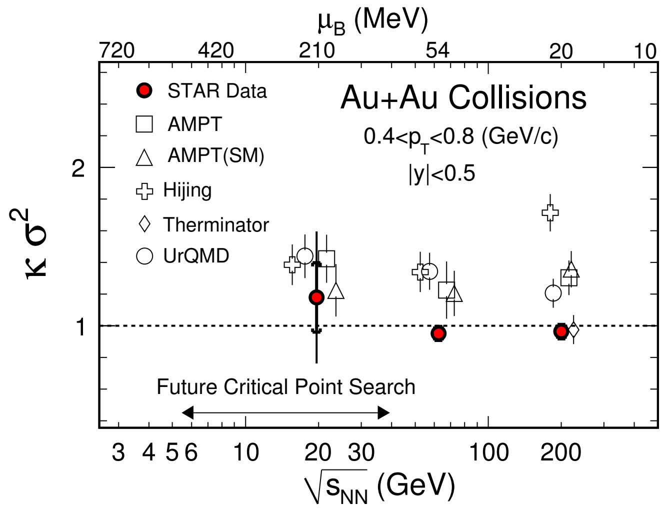

- PRL 105, 022302 (2010)
- Before BES-I
- First attempt

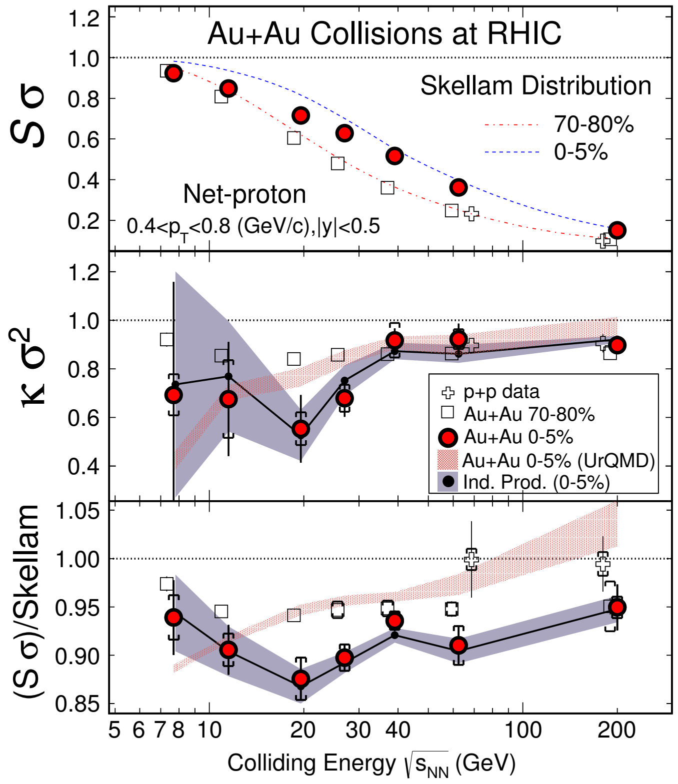

- PRL 112 032302 (2014)
- BES-I (7.7–200 GeV)
- Only low p_T (without TOF)

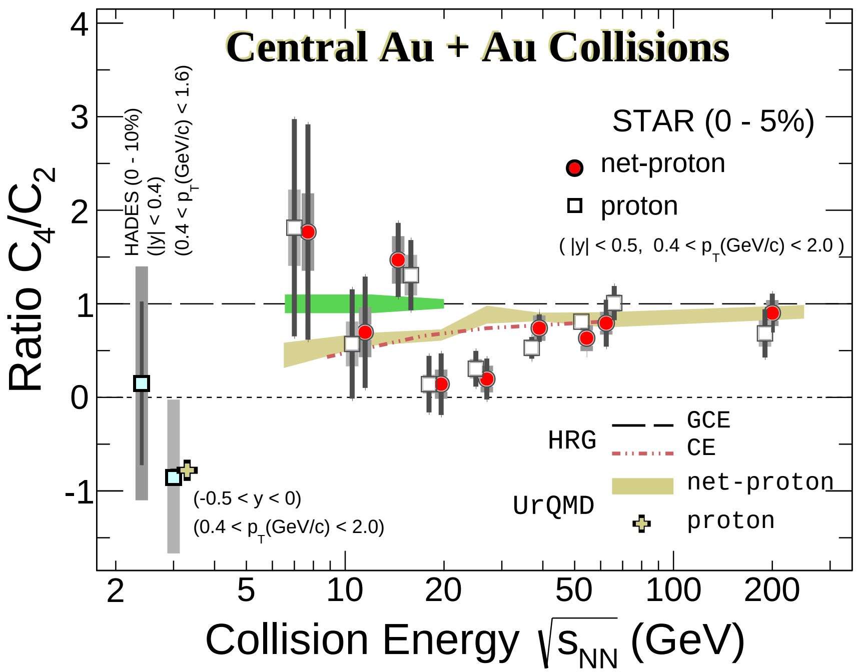

- PRL 126, 092301 (2021)
- PRL 128, 202303 (2022)
- Final results from BES-I and 3 GeV (2018)
- Non-monotonic energy dependence (3.1σ)
- Consistency with UrQMD at 3 GeV

(Net-)Proton Number Fluctuations from 7.7–27 GeV (BES-II Collider Mode)

Since CPOD 2024

Centrality Determination

Two multiplicity definitions with different acceptances

RefMult3		RefMult3X
BES-I	BES-II	BES-II
w/o iTPC	w/ iTPC	w/ iTPC
$\|\eta\| < 1.0$	$\|\eta\| < 1.0$	$\|\eta\| < 1.6$

- Charged-particle multiplicities used for centrality
- (Anti)protons excluded to avoid self-correlation

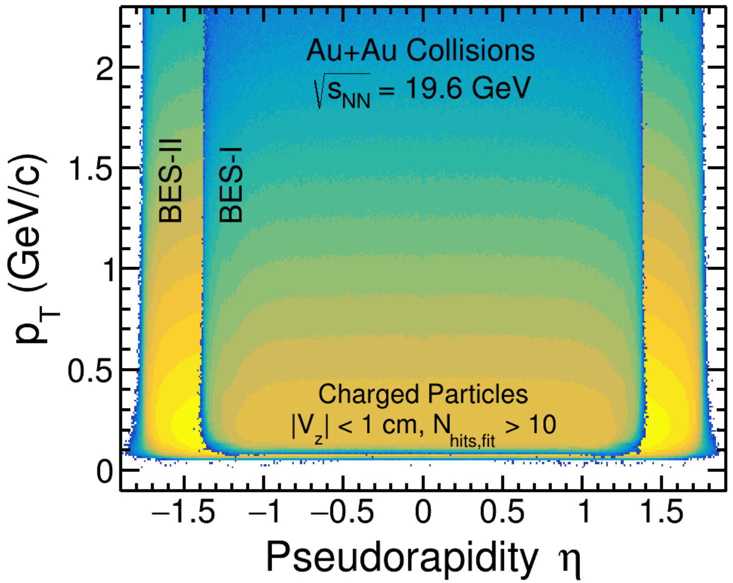

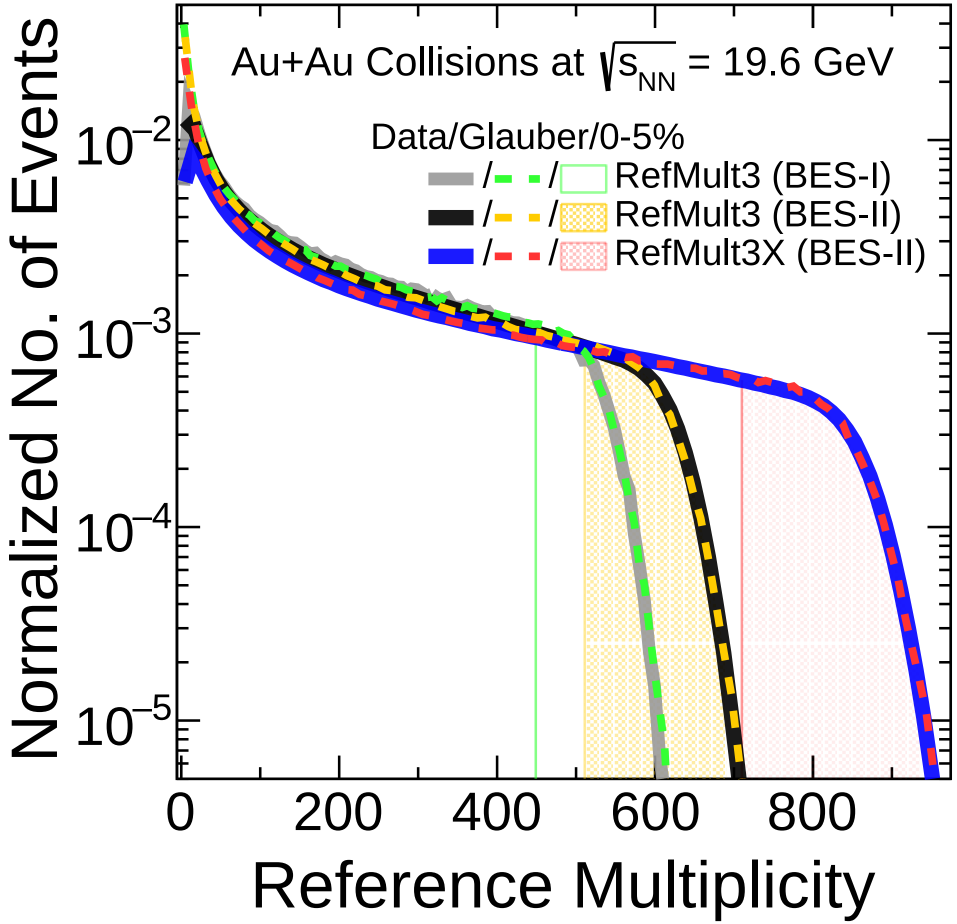

- Larger multiplicity ⇒ better centrality resolution
  - RefMult3 (BES-I) < RefMult3 (BES-II) < RefMult3X

STAR, arXiv:2504.00817

Particle Identification

- (Anti)proton acceptance in this analysis: $0.4 < p_T$ (GeV/c) < 2.0, $|y| < 0.5$

PID selection criteria for protons and antiprotons

p_T (GeV/c)	0.4–0.8	0.8–2.0
Rapidity	$\|y\| < 0.5$	
Detector	TPC	TPC+TOF
TPC dE/dx	$\|n\sigma_{\text{proton}}\| < 2$	
TOF m^2 (GeV^2/c^4)	/	0.6–1.2

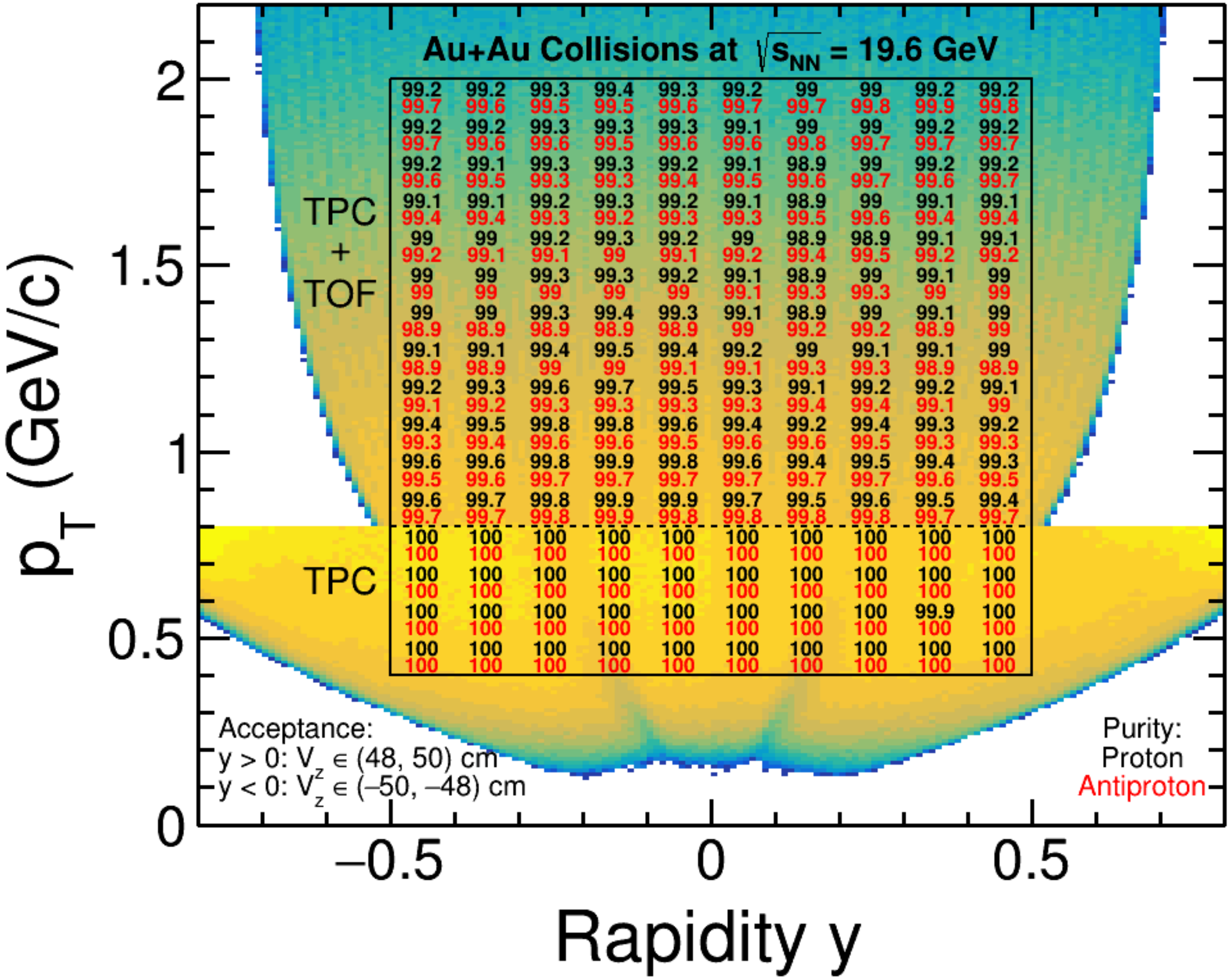

- Uniform (anti)proton acceptance in $|y| < 0.5$ within $|V_z| < 50$ cm
- Bin-by-bin proton/antiproton purity > 99%

A. Pandav (STAR), CPOD 2024
Y. Zhang (STAR), SQM 2024

Improvements in BES-II

1. More collision energies: 9.2 GeV and 17.3 GeV
   - Finer scan of μ_B in the phase diagram

2. Better statistics
   - Event statistics enlarged by a factor of 7–18
   - $\sim$10% higher tracking efficiency from iTPC

3. Better systematics
   - Tracking and PID performance improved by iTPC
   - Efficiency uncertainty suppressed from 5% down to 2%

4. Better centrality resolution
   - Low-p_T tracking enhanced
   - Acceptance expanded

Reduction factor in uncertainties of 0–5% C_4/C_2 in BES-II compared to BES-I

	7.7 GeV	19.6 GeV
Stat.	4.7	4.5
Sys.	3.2	4

STAR, arXiv:2504.00817

Cumulant Ratios vs. Collision Centrality and Energy

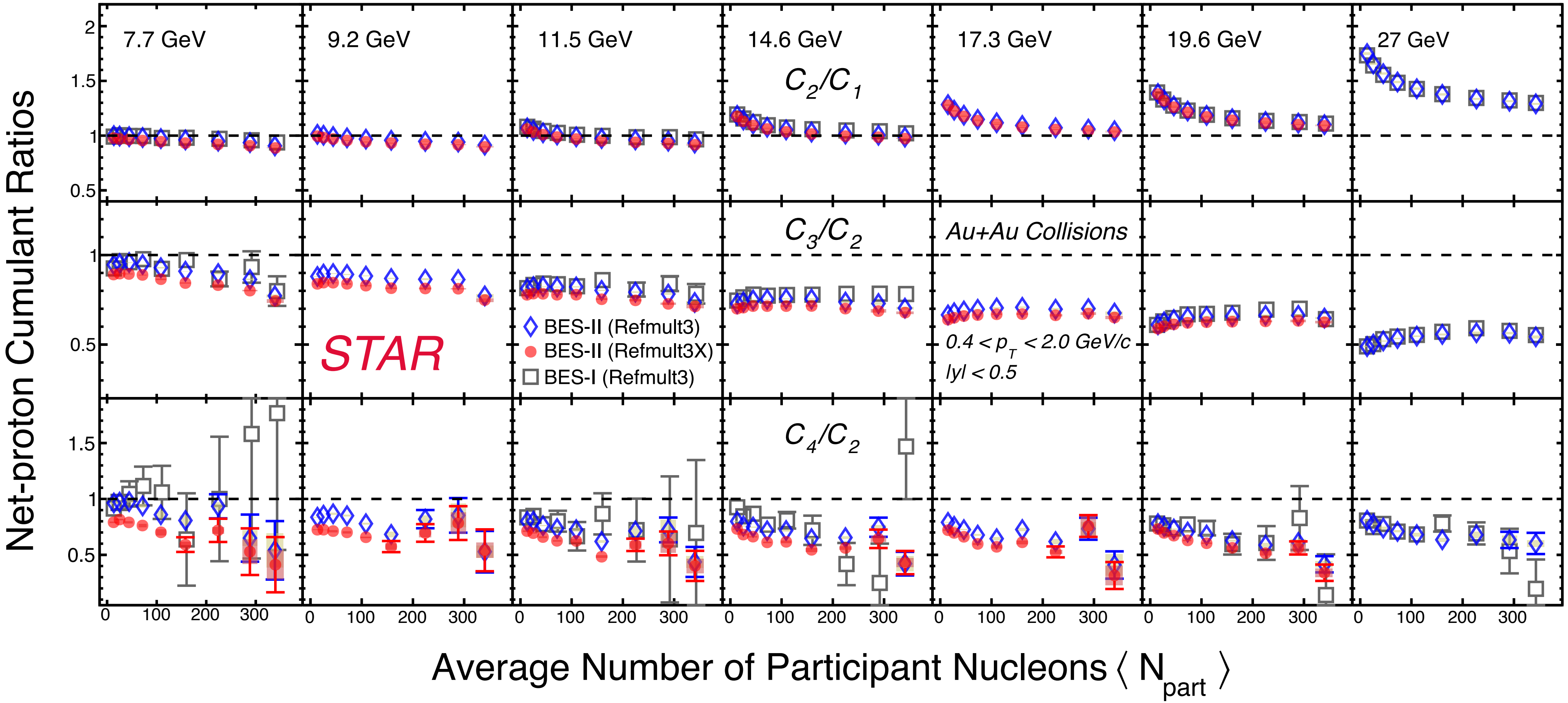

1. Precision measurement of centrality dependence across collision energies
2. Better centrality resolution leads to lower cumulants/ratios (especially in mid-central events)

   Results from RefMult3X (BES-II) < RefMult3 (BES-II) < RefMult3 (BES-I)
3. For 0–5% C_4/C_2, weak effect of centrality resolution

STAR, arXiv:2504.00817

Energy Dependence of Cumulant Ratios

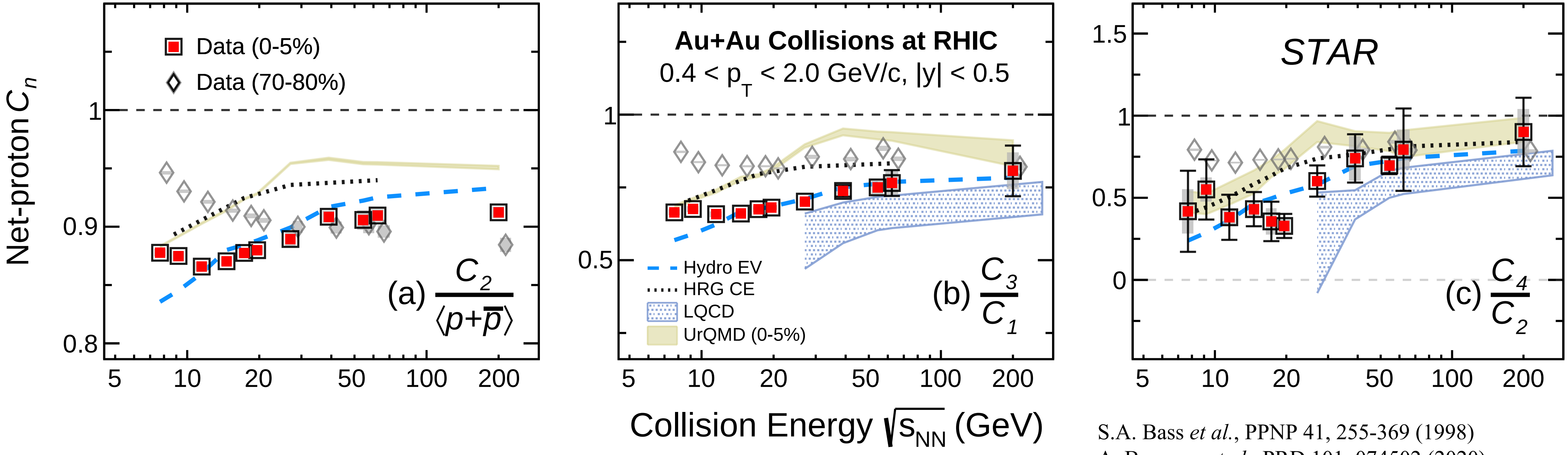

S.A. Bass *et al.*, PPNP 41, 255-369 (1998)
A. Bazavov *et al.*, PRD 101, 074502 (2020)
P. Braun-Munzinger *et al.*, NPA 1008, 122141 (2021)
V. Vovchenko *et al.*, PRC 105, 014904 (2022)
STAR, arXiv:2504.00817

1. High precision in both 0–5% and 70–80%
2. All cumulant ratios below Poisson baseline at unity
3. Peripheral data are closer to unity than central data
4. In central collisions,
   - Decreasing trend as energy decreases, except hint of rising $C_2/\langle p + \bar{p}\rangle$ at low energies
   - C_4/C_2 shows deviation at $\sqrt{s_{NN}} \sim 20$ GeV w.r.t non-CP models (with baryon conservation)

Energy Dependence of Factorial Cumulant Ratios

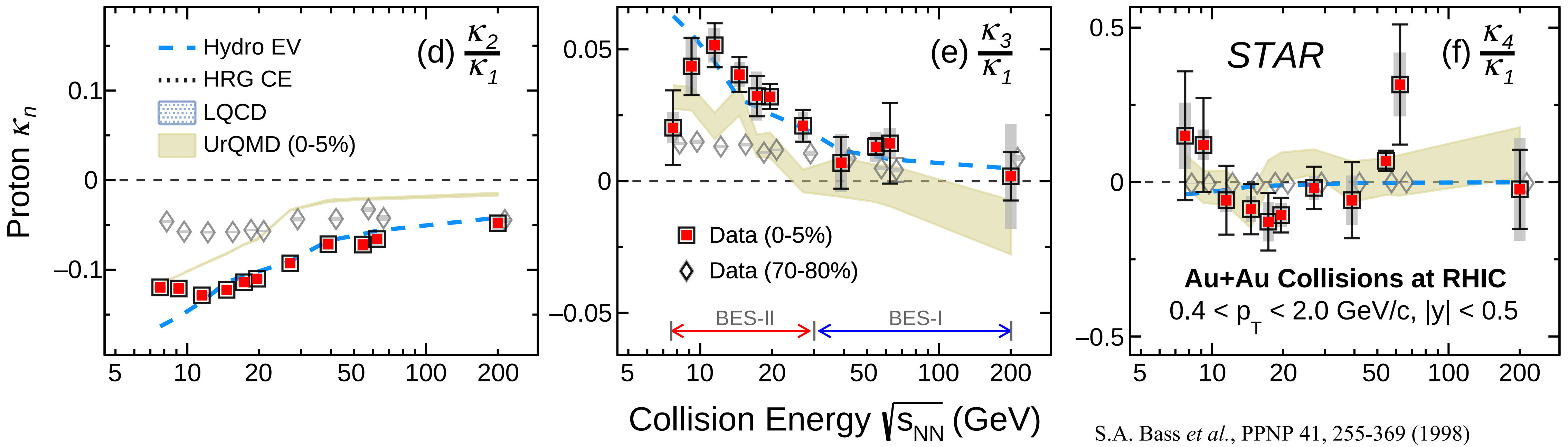

S.A. Bass *et al.*, PPNP 41, 255-369 (1998)
P. Braun-Munzinger *et al.*, NPA 1008, 122141 (2021)
V. Vovchenko *et al.*, PRC 105, 014904 (2022)
STAR, arXiv:2504.00817

1. High precision in both 0–5% and 70–80%
2. Negative κ_2; positive κ_3; κ_4/κ_1 consistent with Poisson baseline at zero within uncertainties
3. Peripheral data are closer to zero than central data
4. In central collisions,
   - κ_2/κ_1 and κ_3/κ_1 show hint of non-monotonic energy dependence, with maximum deviation from zero at $\sqrt{s_{\rm NN}} \sim 11.5$ GeV

Comparison to Theoretical Expectation of CP

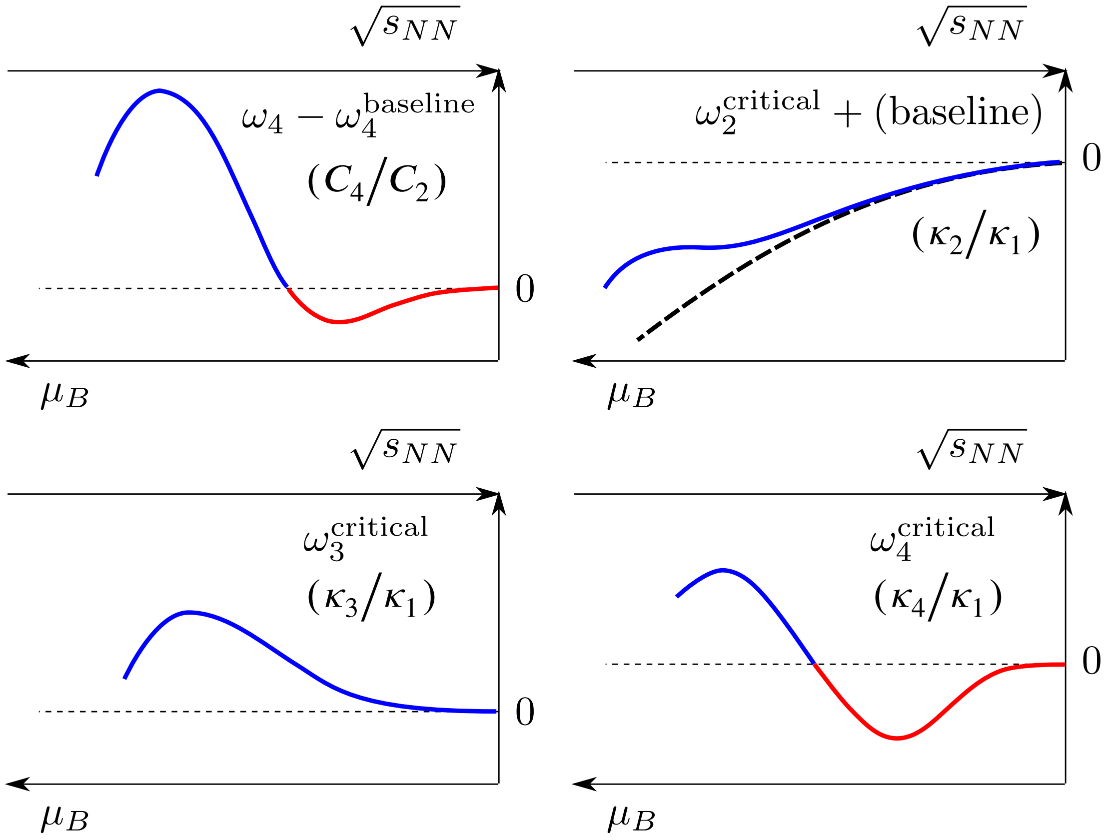

M. Stephanov, Acta Phys.Polon.B 55, 5-A4 (2024)
M. Stephanov, EPJ Web Conf. 314, 00042 (2024)

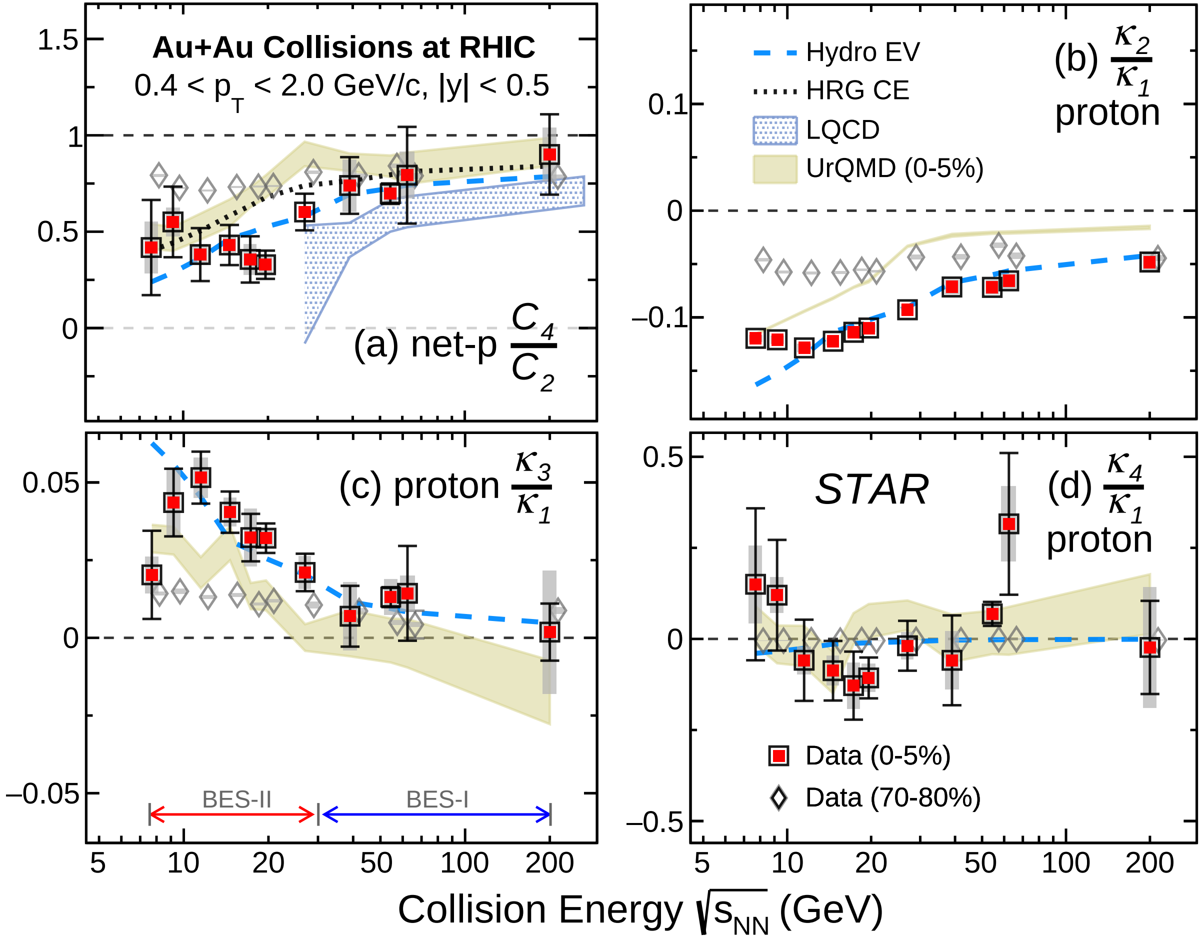

STAR, arXiv:2504.00817

- Qualitative consistency observed
  - (a) C_4/C_2: decreases and reaches a dip at ~19.6 GeV
  - (b) κ_2/κ_1: its decrease likely interrupted below ~11.5 GeV
  - (c) κ_3/κ_1: peak at ~11.5 GeV
  - (d) κ_4/κ_1: dip at ~19.6 GeV, enhancement at lower energy

Deviations between Data and Non-CP References

1. References
   - 3 non-CP models
   - 70–80% data

2. Significance = $\dfrac{0\text{–}5\%\ \text{data} - \text{reference}}{\sqrt{\sigma^2_{0\text{–}5\%\ \text{data}} + \sigma^2_{\text{reference}}}}$

3. For C_4/C_2 (Panel a)
   - All references show a maximum deviation (2–5σ) at 19.6 GeV
   - Data consistent with references at $\sqrt{s_{\mathrm{NN}}} = 3$ GeV and $\gtrsim 27$ GeV

4. For factorial cumulant ratios (Panels b–d)
   - Decreasing deviation as the order increases, considering larger errors

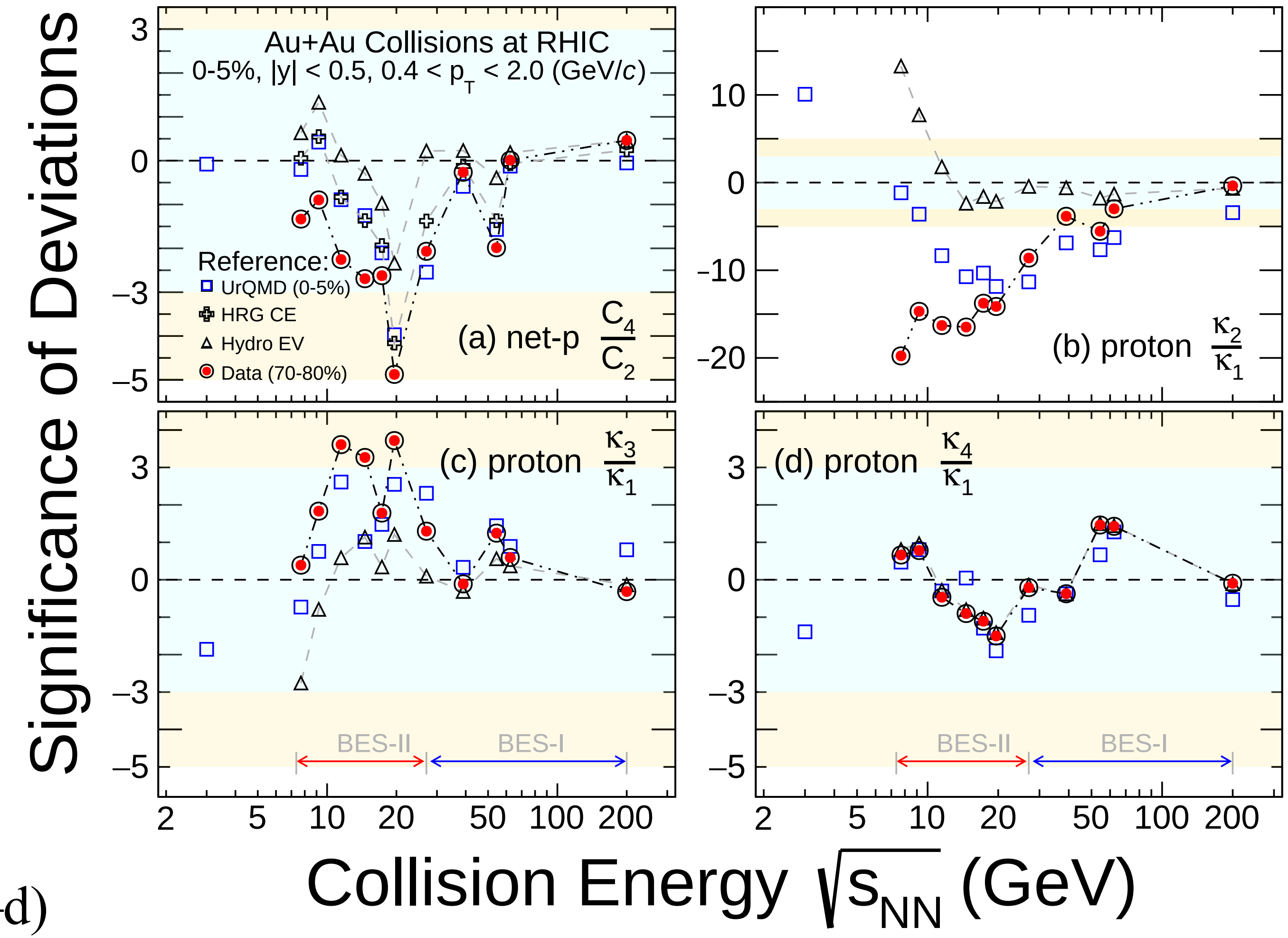

STAR, arXiv:2504.00817

(Net-)Proton Number Fluctuations from 7.7–27 GeV (BES-II Collider Mode)

Since QM 2025

Rapidity Scan of Net-Proton Cumulant Ratios

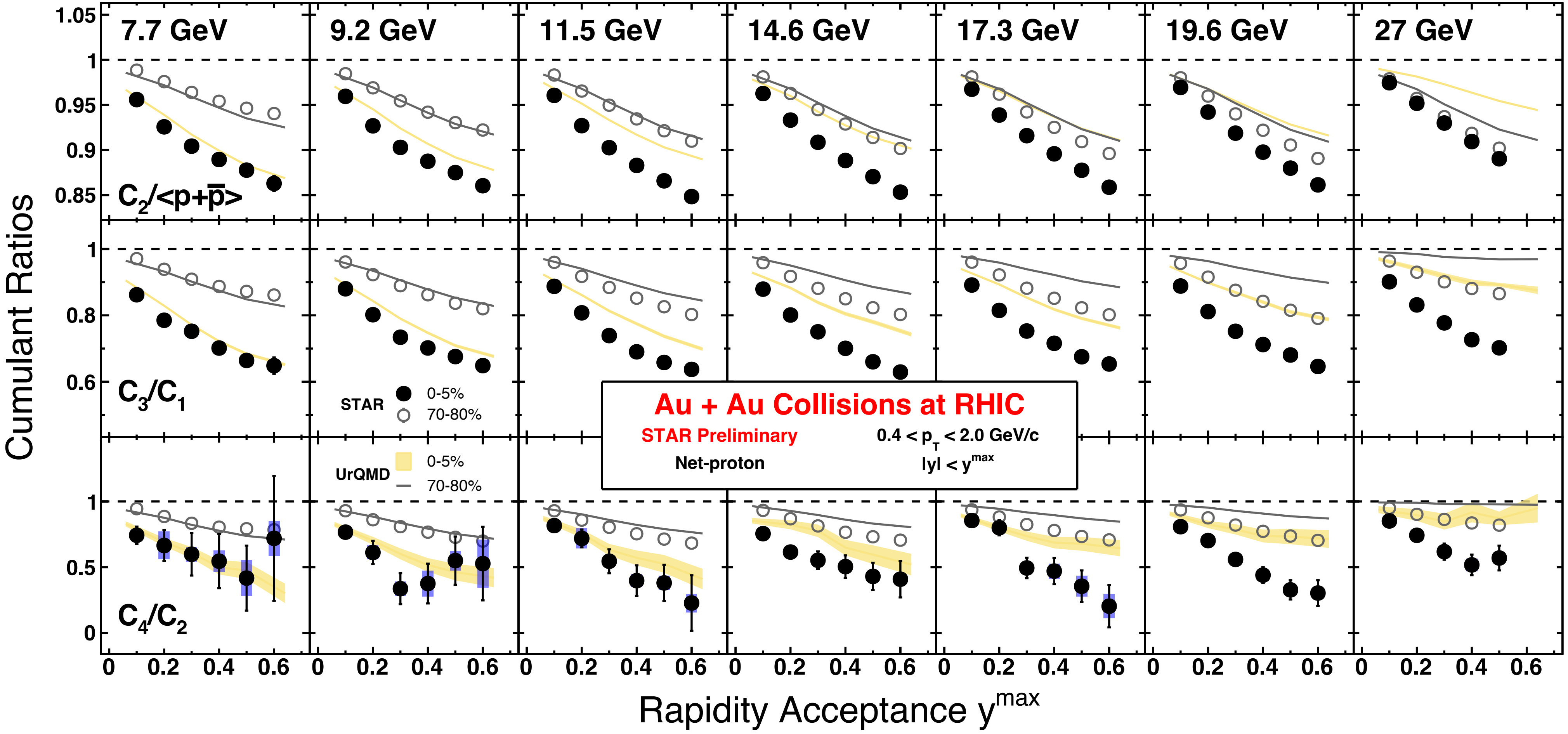

1. Maximum rapidity extended to 0.6 taking advantage of iTPC
2. Decreasing trend as the rapidity window grows
3. UrQMD follows the trend, but deviate quantitatively at higher energies

Y. Huang (STAR), QM 2025

Rapidity Scan of Proton Factorial Cumulant Ratios

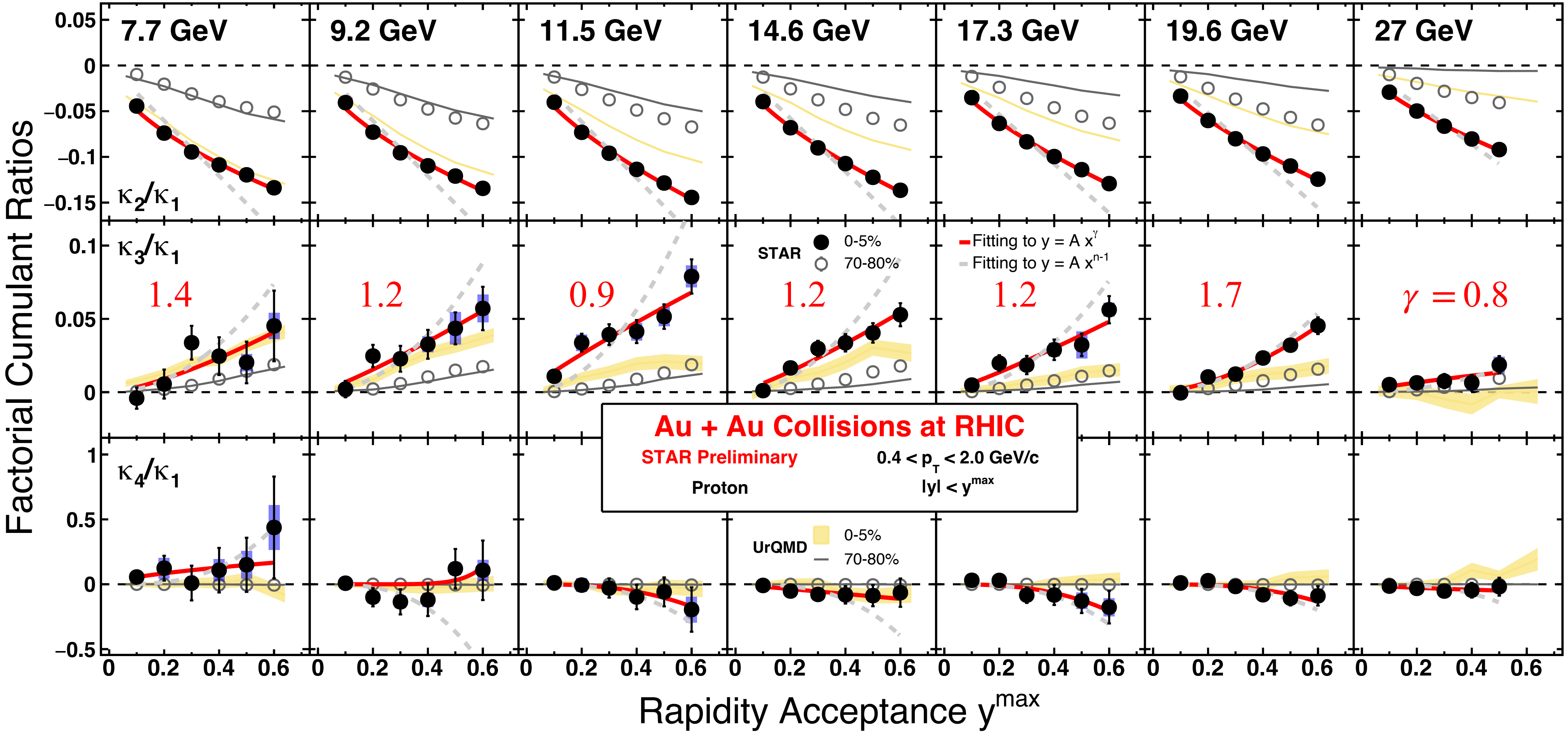

1. Test using parameterization of $\kappa_n/\kappa_1 = A(\Delta y)^{n-1}$ and $A(\Delta y)^{\gamma}$ ($\Delta y = 2y^{\max}$)
2. κ_n/κ_1 follows a power function of Δy
3. The power index lower than expected $(n-1)$ in case of $\Delta y \ll \Delta y_{\mathrm{corr}}$

B. Ling, M.A. Stephanov, PRC 93, 034915, (2016)
Y. Huang (STAR), QM 2025

Finite-Size Scaling (FSS) Study

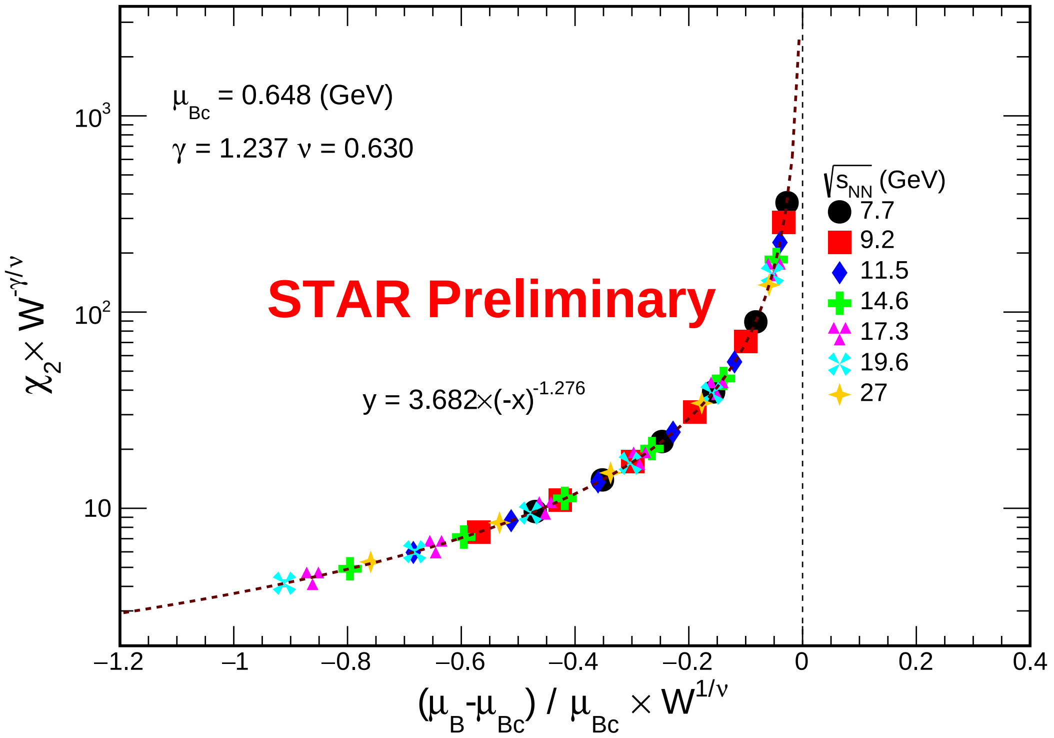

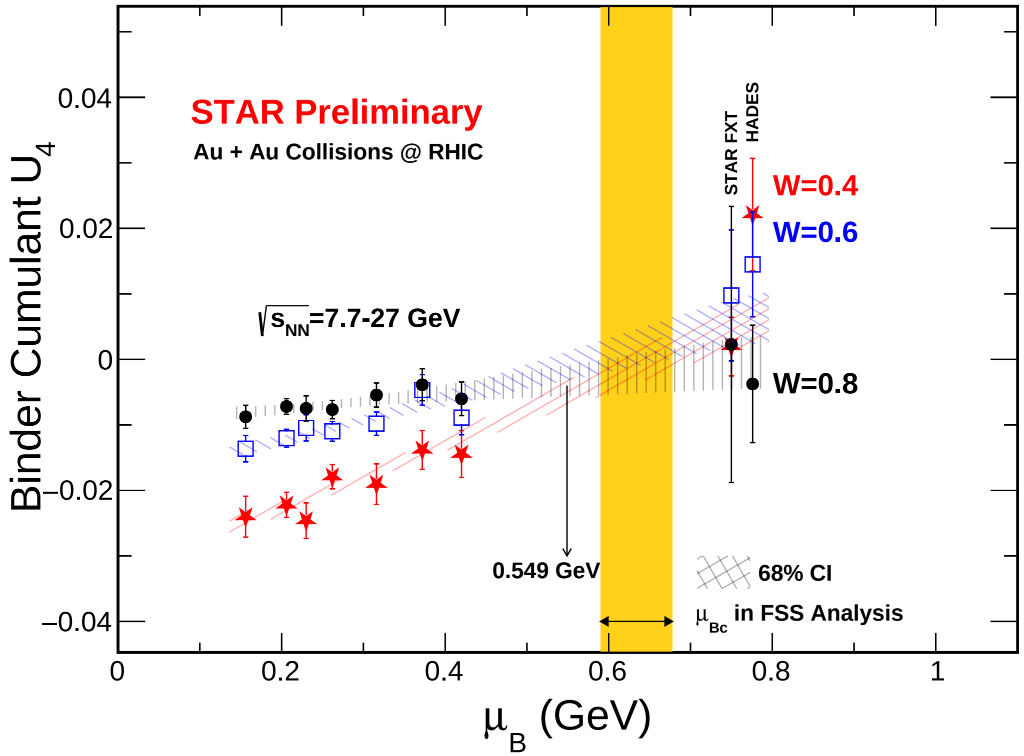

1. FSS study introduces $\mu_{\mathrm{B,c}} = 648^{+30/+2}_{-24/-58}$ MeV from this work
   - $\mu_{\mathrm{B,c}} = 625 \pm 60$ MeV based on BES-I results when FSS proposed
   - Susceptibility $\chi_2(W, \mu_{\mathrm{fo}}) = \dfrac{C_2(W, \mu_{\mathrm{fo}})}{T^3_{\mathrm{fo}} W \, \mathrm{d}V_{\mathrm{fo}}/\mathrm{d}y}$ with rapidity window size W and freeze-out parameters $T, \mu, \mathrm{d}V/\mathrm{d}y$
   - Parameterization uses critical exponents γ, ν
2. Linear fits for binder cumulants $U_4 = -3\, C_4/C_2^2$ provide an overlapping μ_{B} region consistent with FSS

HADES, PRC 102, 024914 (2020)
STAR, PRC 107, 024908 (2023)
A.Sorensen, P.Sorensen, arXiv:2405.10278
Y. Huang (STAR), QM 2025

Proton Number Fluctuations from 3.2–3.9 GeV (BES-II FXT Mode)

Since QM 2025

Proton Acceptance

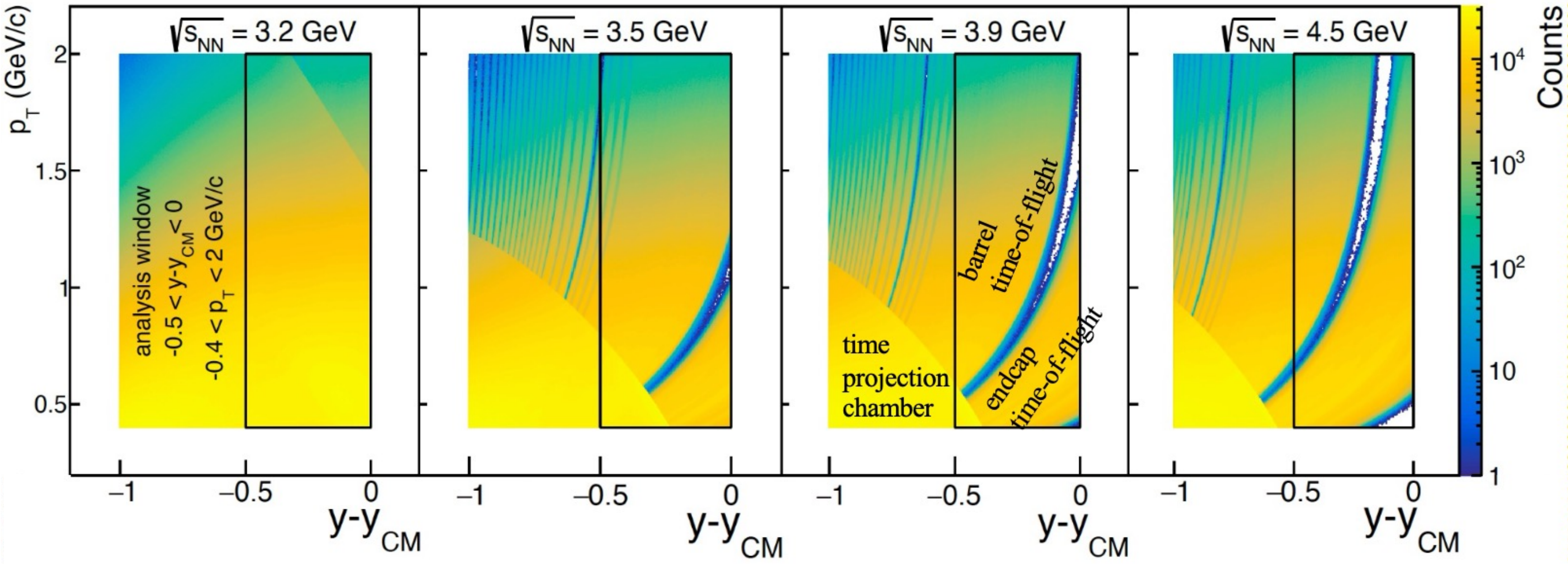

⇐ Conventional selection:

- TPC PID at low *p*
- TPC+TOF at high *p*

Z. Sweger *et al.*, PRC 111, 034902 (2025)
Z. Sweger (STAR), QM 2025

- TOF improves purity but reduces acceptance coverage and efficiency
- A gap between bTOF and eTOF contributes more to the mid-rapidity window at higher energy
- In case of mixed use of slow (TPC) and fast (TOF) detectors, pileup distorts the measured fluctuations and cannot be corrected for

Proton Acceptance

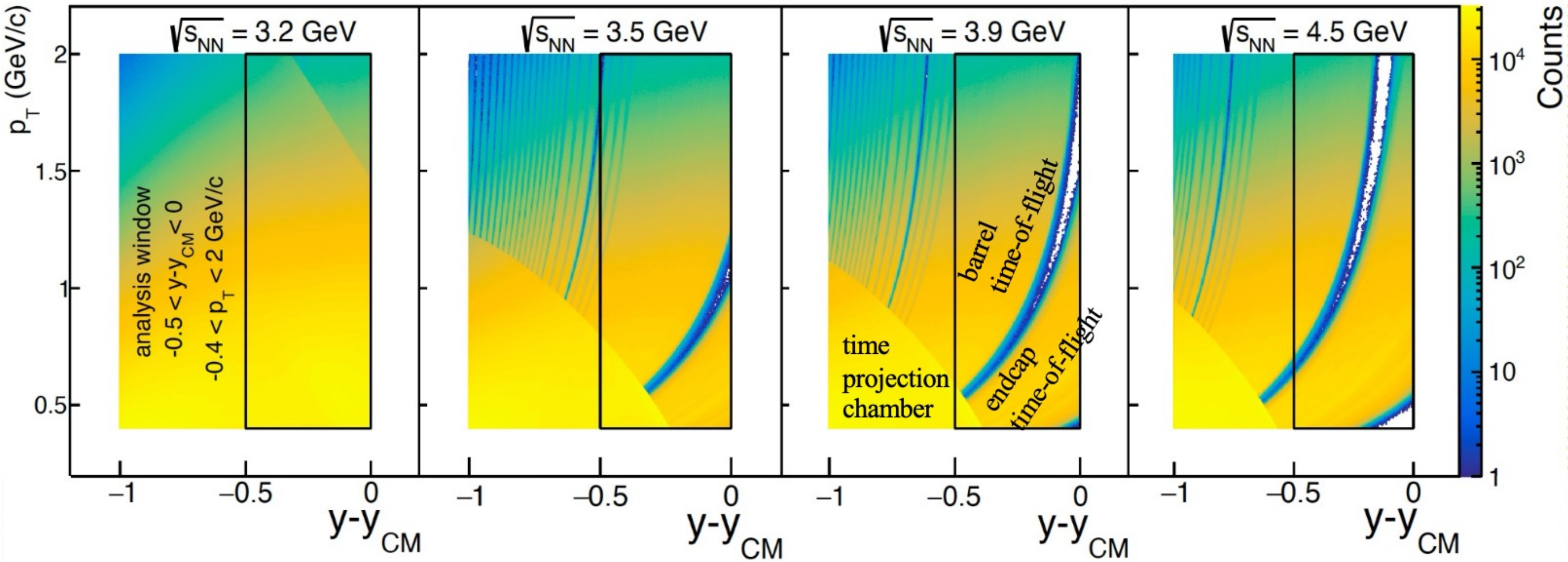

⇐ Conventional selection:

- TPC PID at low *p*
- TPC+TOF at high *p*

Z. Sweger *et al.*, PRC 111, 034902 (2025)
Z. Sweger (STAR), QM 2025

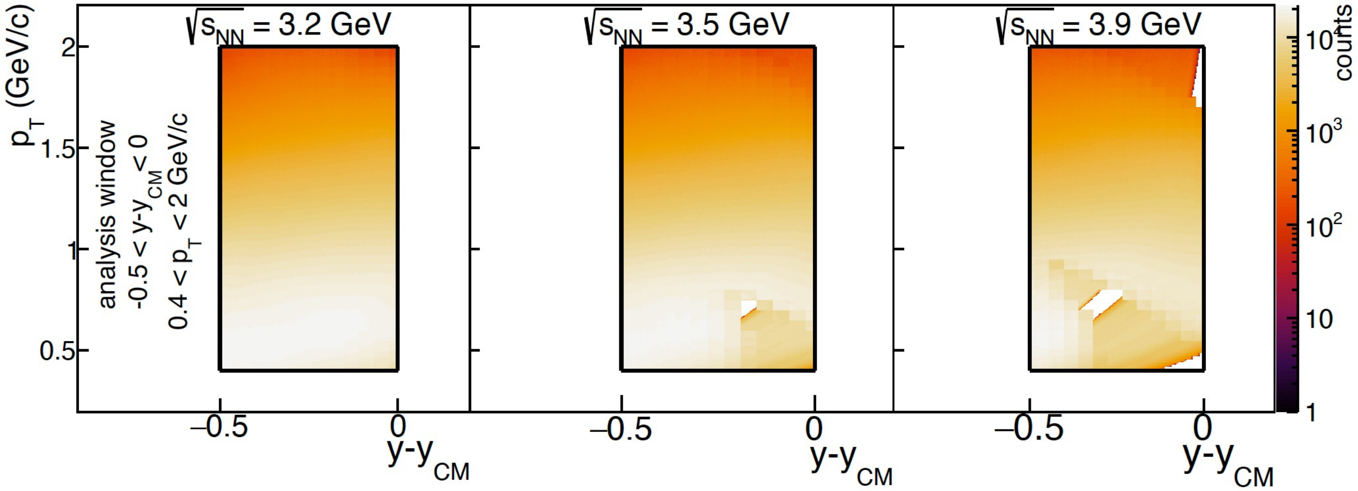

⇐ Strategy in this work:

- Ensure purity > 90% and maximize TPC PID by dynamic $n\sigma_{\text{proton}}$ cut
- TOF is used where purity cannot reach 90%
- 3.2 GeV: TOF is not required, and pileup correction is done
- 3.5 and 3.9 GeV: TOF is required, and pileup rejection is done

Centrality Determination

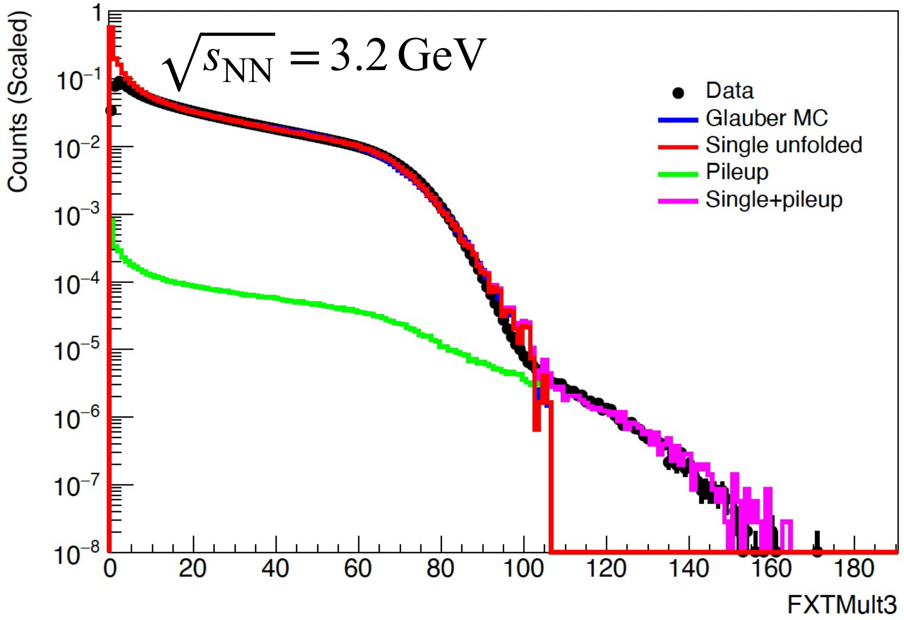

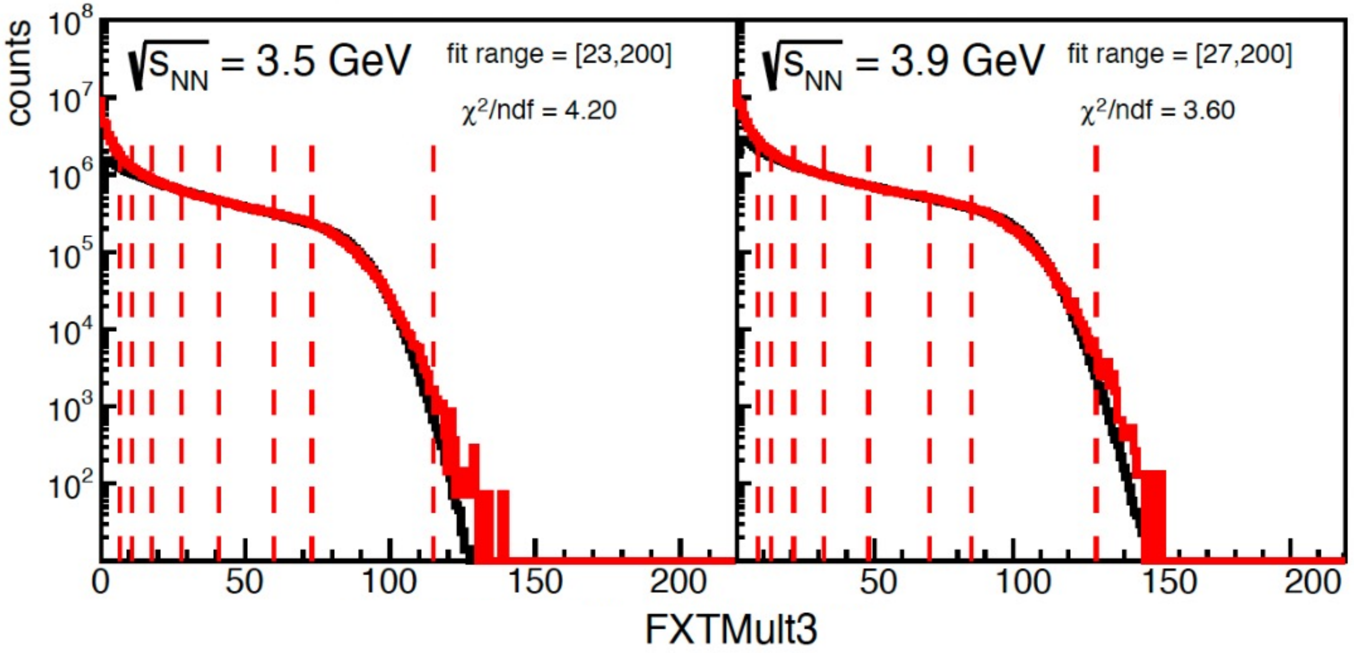

- FXTMult3: multiplicity of charged particles with no η cut, including
  - All negatively charged particles
  - Low-momentum positively charged particles excluding protons

Z. Sweger (STAR), QM 2025

Energy Dependence of (Factorial) Cumulant Ratios

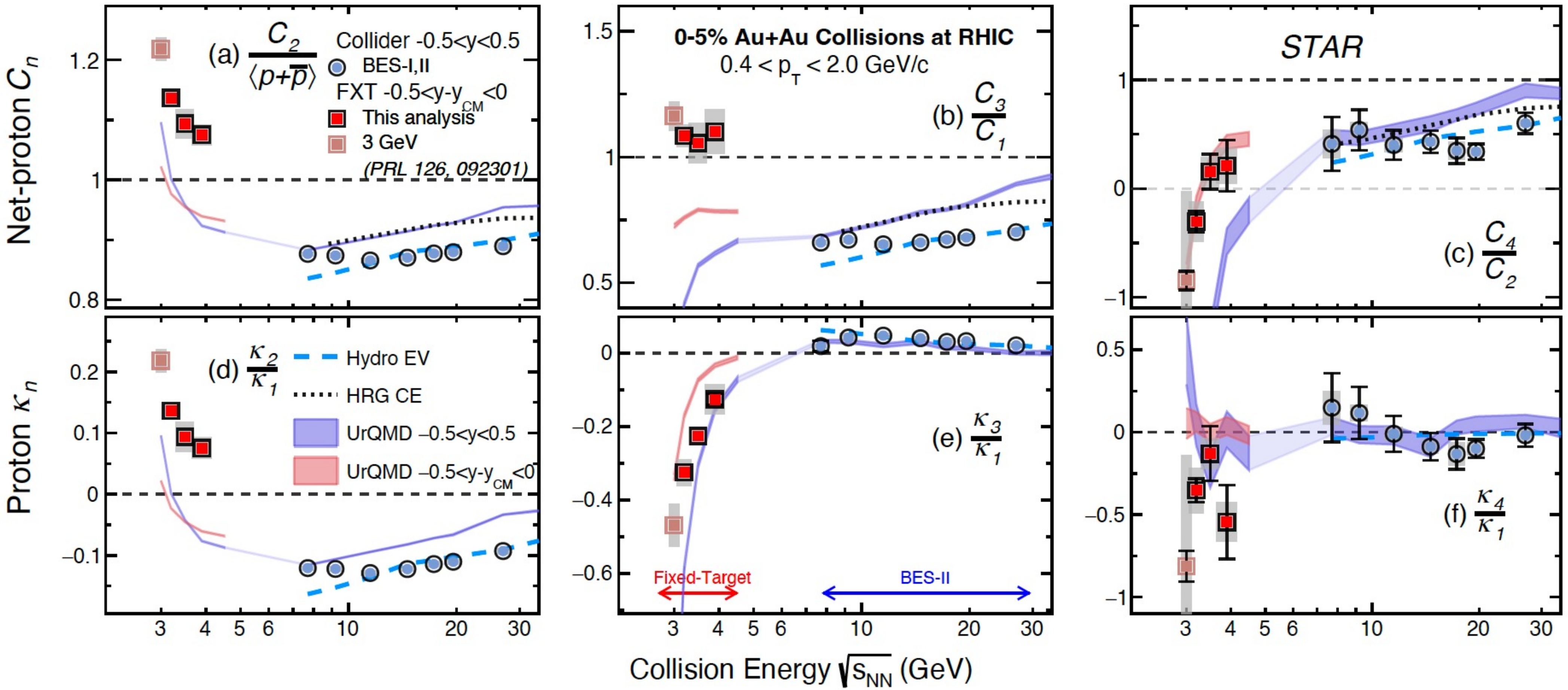

1. Decreasing C_2/C_1 and κ_2/κ_1, increasing C_4/C_2 and κ_3/κ_1 as energy increases
2. UrQMD calculations for half mid-rapidity (including acceptance gap) and full mid-rapidity reproduce trends of data
3. C_4/C_2 agrees well with UrQMD, while 2nd and 3rd orders show clear deviations

Z. Sweger (STAR), QM 2025

Significance of Deviations from References

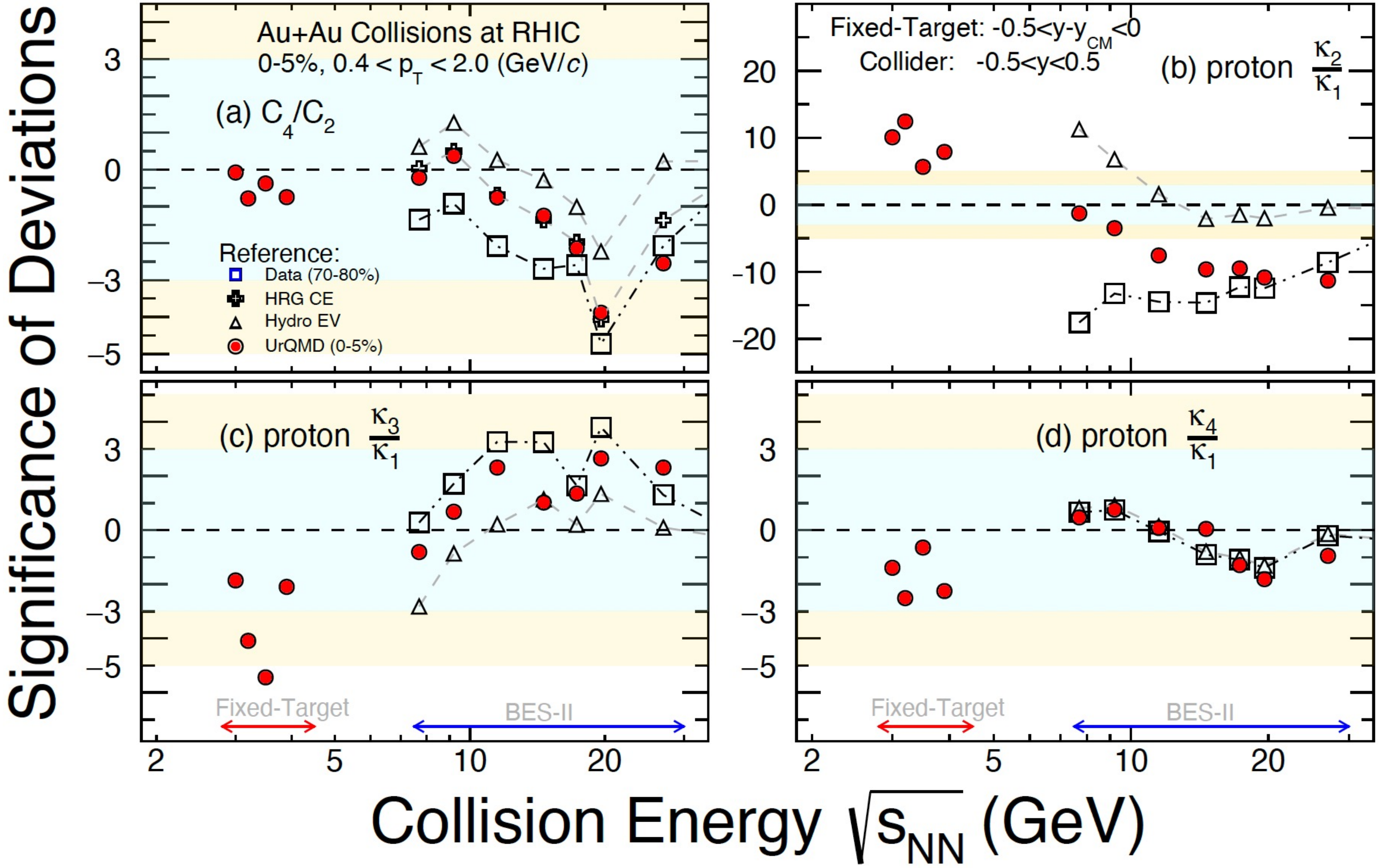

- Significant deviations of κ_2/κ_1 and κ_3/κ_1 from UrQMD
- C_4/C_2 deviates within 1σ, and κ_4/κ_1 deviates within 3σ

Z. Sweger (STAR), QM 2025

Summary

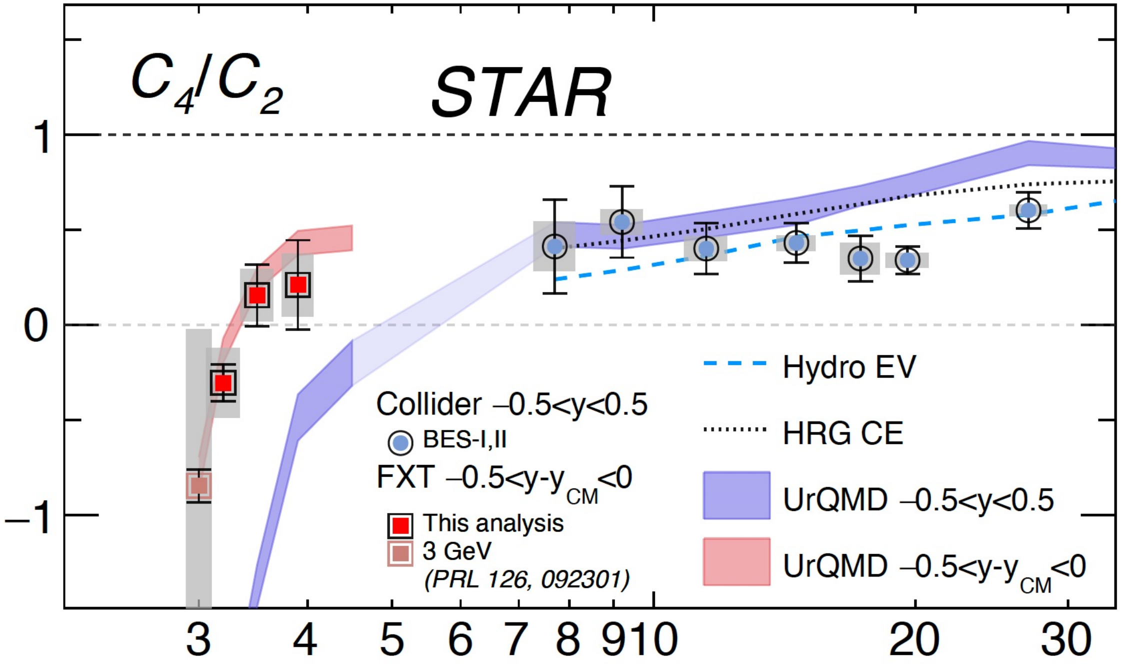

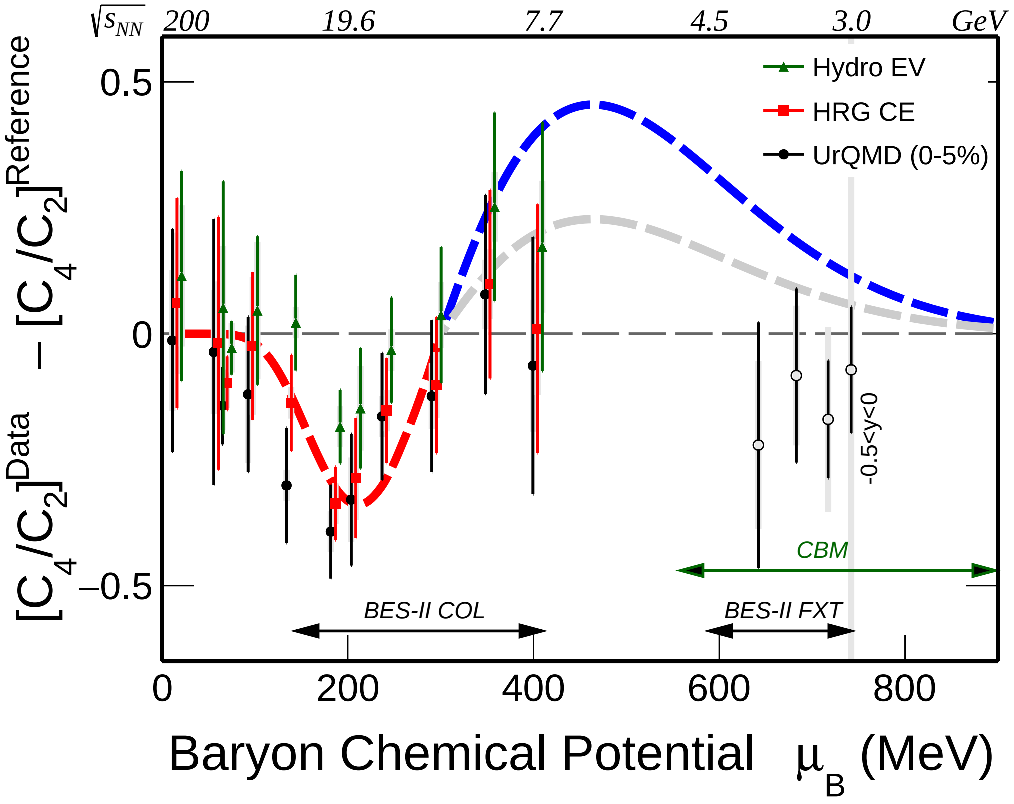

1. Precision measurement of (net-)proton number fluctuations in Au+Au collisions at $\sqrt{s_{NN}}$ = 3.2–3.9 GeV and 7.7–27 GeV from RHIC-STAR BES-II
2. Compared to non-CP refs., central C_4/C_2 shows a max. deviation at $\sqrt{s_{NN}} \sim 20$ GeV (2–5σ).
3. FSS and Binder cumulant studies introduce an interesting region of $\mu_B \sim 600$ MeV.

Outlook: Other Observables

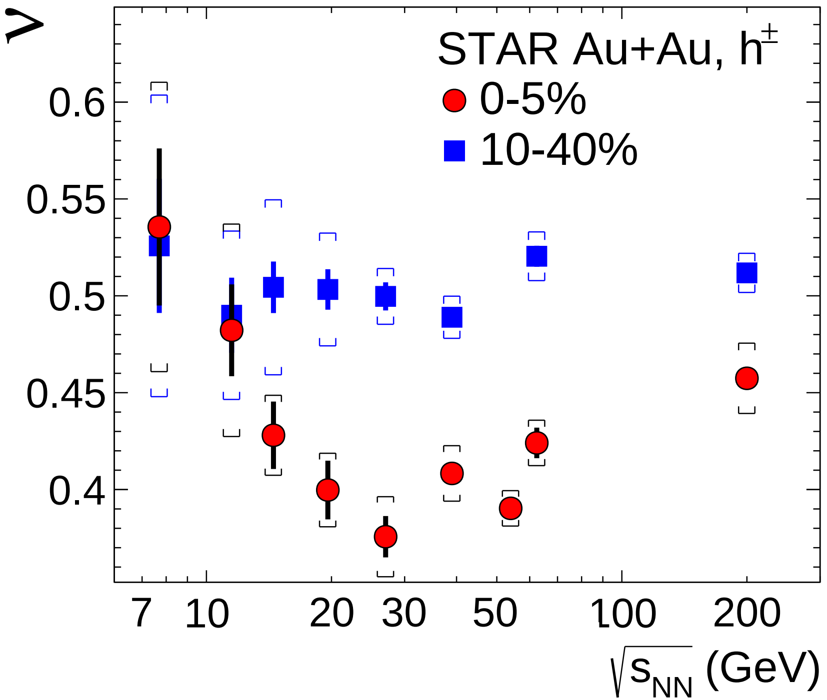

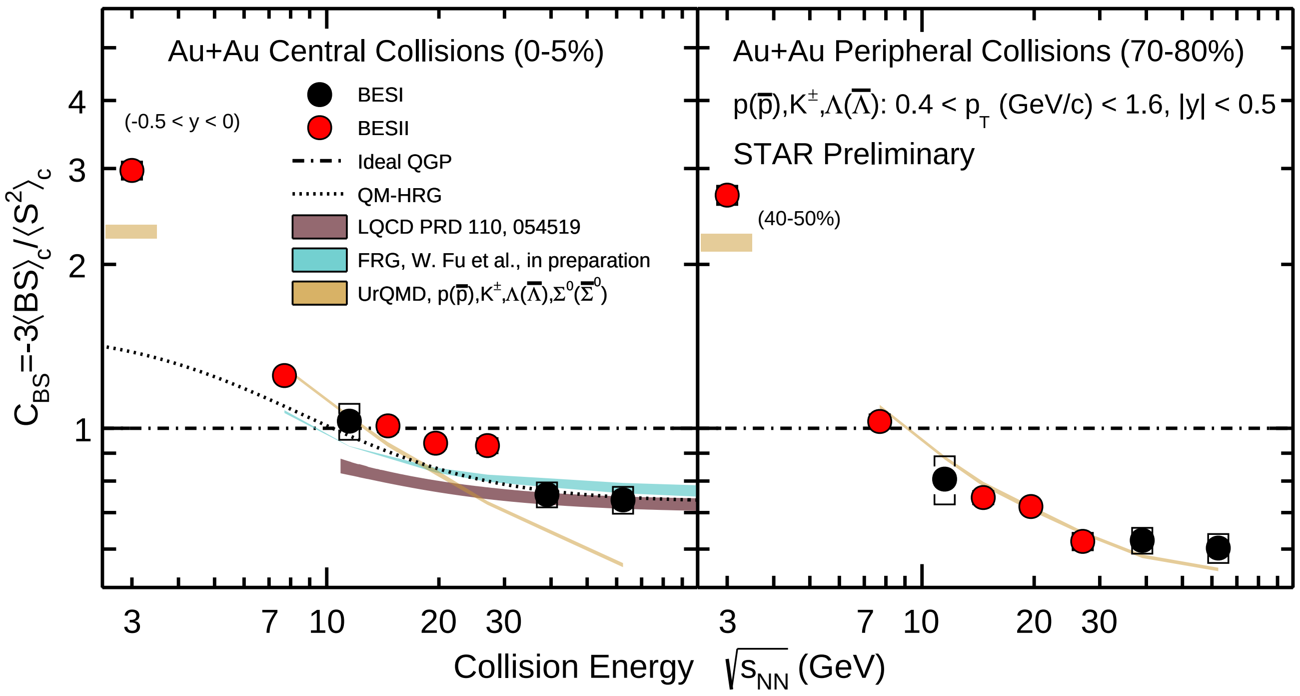

- Charged-hadron intermittency (ν): BES-I
- Baryon-strangeness correlation (C_{BS}): BES-I/II
- Non-monotonic behavior or deviation from references around 20 GeV

STAR, PLB 845, 138165 (2023)
H. Feng (STAR), QM 2025

Outlook: Future Facilities/Experiments

- Crucial for high baryon density
  - NICA-MPD in Russia:
    $\sqrt{s_{\mathrm{NN}}} \sim 4\text{–}11$ GeV,
    $\mu_B \sim 620\text{–}330$ MeV
  - HIAF-CEE+ in China:
    $\sqrt{s_{\mathrm{NN}}} \sim 2.1\text{–}4.5$ GeV,
    $\mu_B \sim 830\text{–}590$ MeV
  - FAIR-CBM in Germany:
    $\sqrt{s_{\mathrm{NN}}} \sim 2.3\text{–}5.3$ GeV,
    $\mu_B \sim 800\text{–}530$ MeV
  - J-PARC-HI in Japan:
    $\sqrt{s_{\mathrm{NN}}} \sim 2\text{–}6.2$ GeV,
    $\mu_B \sim 850\text{–}490$ MeV

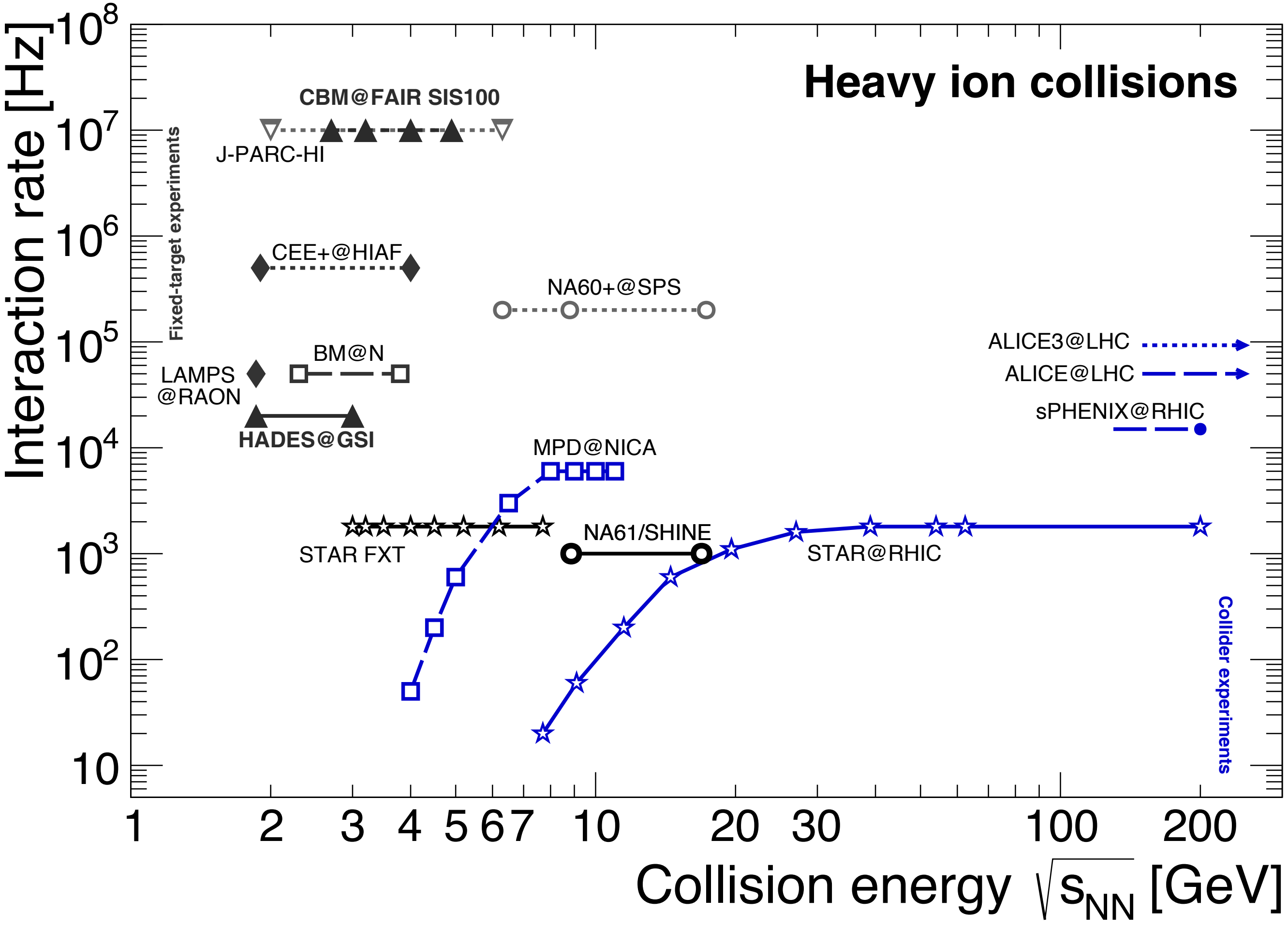

C. Höhne (CBM), EPJ Web Conf. 296, 08004 (2024)

Acknowledgements

Alphabetically: Daniel Cebra, Xin Dong, ShinIchi Esumi, Yige Huang, Xiaofeng Luo, Bedangadas Mohanty, Bappaditya Mondal, Toshihiro Nonaka, Ashish Pandav, Zachary Sweger, Zhaohui Wang, Nu Xu, Yongcong Xu, Xin Zhang, Yifei Zhang, Yu Zhang and the STAR Collaboration

Thanks to organizers for this opportunity.

Thank you all for your attention!